REVISTA IBRACON DE ESTRUTURAS E MATERIAIS

IBRACON STRUCTURES AND MATERIALS JOURNAL

Analysis of the nodal stresses in pile caps

Análise das tensões nodais em blocos sobre estacas

M. A. TOMAZ [a]
eng.matomaz@gmail.com

R. G. DELALIBERA [a]
delalibera@ufu.br

J. S. GIONGO [b]
jsgiongo@sc.usp.br

V. F. GONÇALVES [a]
vitorfrg@gmail.com

Abstract

Pile caps can be dimensioned using, preferably, plastic models (strut-and-tie) and models based on the flexion theory. In order to analyze the behavior of the stresses in the lower and upper nodal regions of the cap, a theoretical analysis of the experimental results found by several researchers was made. There was a discrepancy in the results obtained and, as a result, a critical analysis carried out and a new methodology for the verification of the nodal stress near the upper zone, based on the multiaxial behavior of the concrete, is suggested.

Keywords: pile caps, strut-and-tie model, nodal stress.

Resumo

Blocos sobre estacas podem ser dimensionados utilizando-se, preferencialmente, modelos plásticos (bielas e tirantes) e modelos baseados na teoria da flexão. Com o intuito de analisar o comportamento das tensões nas regiões nodais inferior e superior do bloco, fez-se uma análise teórica dos resultados dos ensaios experimentais realizados por diversos pesquisadores. Observaram-se divergências nos resultados e, em função disto, foi feita uma análise crítica que permitiu a sugestão de uma nova metodologia para a verificação das tensões nodais junto a zona nodal superior, baseada no comportamento multiaxial do concreto.

Palavras-chave: blocos sobre estacas, modelo de bielas e tirantes, tensões nodais.

[a]   Universidade Federal de Uberlândia, Faculdade de Engenharia Civil, Uberlândia, MG, Brasil;
[b]   Universidade de São Paulo, Escola de Engenharia de São Carlos, Departamento de Engenharia de Estruturas, São Carlos-SP, Brasil.

1. Introduction

For pile caps design it is possible to adopt three-dimensional calculation models (linear or not) and strut-and-tie models, the latter being the most indicated because it considers regions of stress discontinuities.

The strut-and-tie model is a method based on the lower bound theory, using the concept of plasticity and consists of the design by idealizing a space truss, composed by connecting struts (representing compression fields), ties (representing tensile fields) and nodes (volume of concrete with the purpose of transfering the stress between connecting struts and ties, and between cap and piles and column and cap). The design consists on verifying the stress on the contact region between the column/pile cap (upper nodal area) and cap/piles (lower nodal area).

Blévot [1] studied the behavior of caps on three and four piles, proposing equation for the models. Blévot and Frémy [2] then extended the study of pile caps, which led them to propose an interval to the angle between the strut and the horizontal axis, in order to ensure that the pile cap is safe. In addition, the authors have suggested maximum values for the stress on the nodal areas. Due to its importance and comprehensiveness, these works have guided all subsequent studies about pile caps.

Since then, the subject has been widely studied and several researchers have proposed different values for the limits of nodal stresses, as well as different ways of applying the strut-and-tie model.

1.1 Justification

The ABNT NBR 6118:2014 [3] does not present specific criteria for the pile caps design, however, it indicates the use of the strut-and-tie model for describing well the internal structural behavior of pile caps.

According to the ABNT NBR 6118:2014 [3], the stresses that arise in the nodal areas should be limited, however, there are many divergences in relation to the criteria adopted by the Brazilian norms and international norms. Likewise, there are also divergences in relation to defining the area and shape of the lower and upper nodal zones.

The Brazilian norm provides parameters for stress verification but it does not specify which strut-and-tie model should be adopted, allowing the engineer to freely choose the most suitable model.

Thus, this article is justified by the uncertainties still existing on the design and verification of pile caps.

1.2 Objective

The purpose of this work was to analyze the nodal stresses obtained through experimental tests, comparing them with the existing normative limits. Methods proposed by different authors for obtaing the nodal stresses were used. Finally, it was aimed to present a criterion considering the multiaxial effect of the concrete near the upper nodal zone.

2. Experimental results used

Firstly, the largest possible number of experimental data was collected regarding the geometric and physical properties of the pile caps (dimensions, distance between pile centers, pile and column cross sections, force applied to the column in which the first crack arose and column reinforcement rates) and the ultimate forces for each cap tested and their respective concrete compressive strength (f_c). Only the pile caps with monolithic connections were considered, in other words, caps with calyx foundation were discarded.

Adebar et al. [4] tested six caps, five of which were supported on four piles and only one supported on six piles, see Figure [1]. The caps on four piles have hexagonal geometry and therefore has two directions (hence the indication of values in the x and y directions). Since model C has six piles, the indication of θ_x refers to the angle of strut related to the most remote pile, and θ_y refers to the angle of the strut related to the nearest pile.

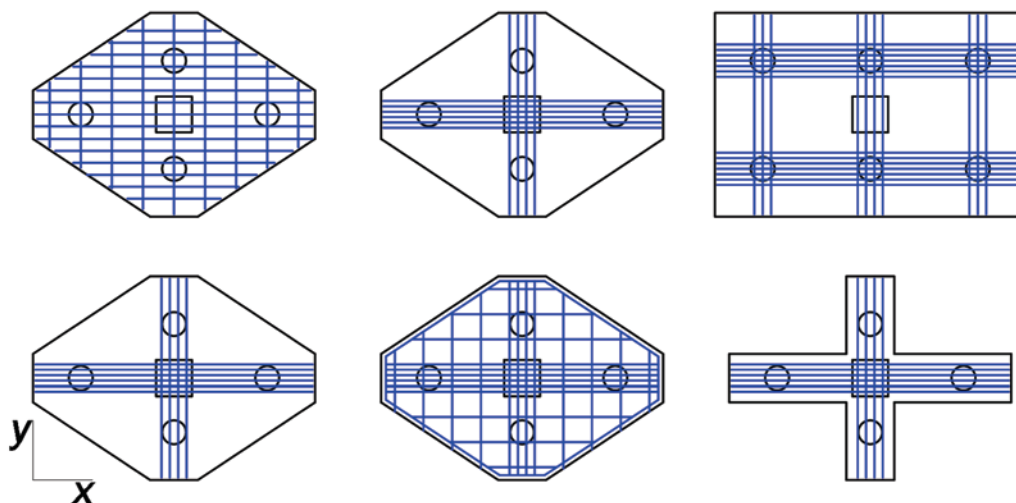The adopted angles were those described as being the observed

Figure 1
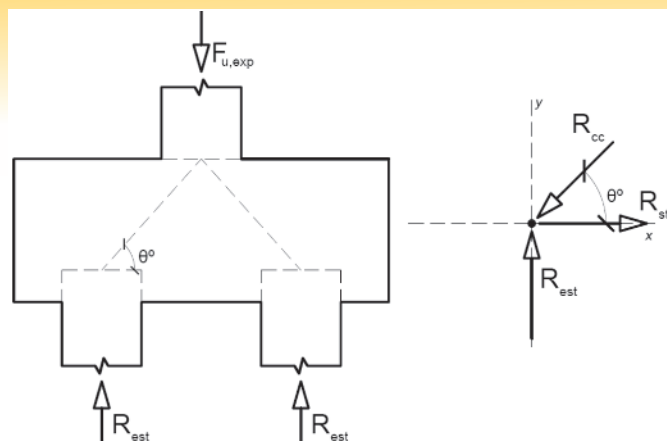Models tested by Adebar *et al.* [4]

Figure 2
Equilibrium of forces in the lower nodal region for R_{st} calculation (resulting force in the tie) and R_{cc} (resulting force in the strut)

angles in the tests. In the cases in which it was not possible to obtain the angle experimentally, a line was drawn by joining the center of gravity of the cross section of the column to the center of gravity of the cross section of the pile. It is important to note that this hypothesis of considering the angle of inclination of the strut in relation to the horizontal plane differs from the model proposed by Blévot and Frémy [2]. The french researchers consider that the beginning of the strut, next to the upper nodal zone, occurs at ¼ of the column size in the considered direction, measured from the column face.

The collected data for the analysis was extracted from the works of Adebar et al. [4], Mautoni [5], Fusco [6], Chan and Poh [7], Miguel [8], Delalibera and Giongo [9], Barros [10], Munhoz [11], Mesquita [12] and Cao and Bloodworth [13] and are shown in Tables [1] to [10].

It is also important to clarify that the experimental tests of Blévot and Frémy [2] were not considered in this work due to the large number of tests. Therefore, the authors of this article decided to elaborate an article similar to this one, considering only the tests of Blévot and Frémy [2].

The purpose of this study was to calculate the nodal stresses, using three different models: Blévot and Frémy [2], Schlaich and Schäfer [14] and Fusco [15]. The models are based on the forces acting on the struts and/or the piles reactions. To calculate such forces, the equilibrium of the nodal region was made as it is shown in Figure [2]. The presence of a bending moment at the base of the column was studied by Delalibera and Giongo [9].

Table 1
Properties of the pile caps analyzed by Mautoni [5]

Tested model	Pile number	Height (cm)	Length (cm)	Pile section (cm×cm)	Distance between piles (cm)	Column section (cm×cm)	Column reinforcement rate (%)	θ (°)	$f_{c,exp}$ (MPa)
B1-1	2	23	50	10×15	31	15×15	–	56.02	21.50
B2-1	2	23	50	10×15	31	15×15	–	26.02	21.50
B1-2	2	23	50	10×15	32	15×15	–	55.18	15.00
B2-2	2	23	50	10×15	32	15×15	–	55.18	15.00
B1-A	2	23	50	10×15	32	15×15	–	55.18	32.30
B2-A	2	23	50	10×15	32	15×15	–	55.18	32.30
B1-B	2	20	50	10×15	32	15×15	–	51.34	32.00
B2-B	2	20	50	10×15	32	15×15	–	51.34	32.00
B1-4A	2	20	50	10×15	32	15×15	–	51.34	29.50
B2-4A	2	20	50	10×15	32	15×15	–	51.34	29.50
B1-4B	2	20	50	10×15	32	15×15	–	51.34	27.80
B2-4B	2	20	50	10×15	32	15×15	–	51.34	27.80
B1-4C	2	20	50	10×15	32	15×15	–	51.34	22.20
B2-4C	2	20	50	10×15	32	15×15	–	51.34	22.20
D1	2	21	50	10×15	35	15×15	–	50.19	22.90
D2	2	21	50	10×15	35	15×15	–	50.19	22.90
F1	2	20	50	10×15	40	15×15	–	45.00	23.60
F2	2	20	50	10×15	40	15×15	–	45.00	23.60
E1	2	20	50	10×15	45	15×15	–	41.63	19.50
G1	2	20	50	10×15	45	15×15	–	41.63	24.30

Note: all pile caps were 15 cm wide.

Table 2
Properties of the pile caps analyzed by Fusco [6]

Tested model	Pile number	Height (cm)	Length (cm)	Pile section (cm×cm)	Distance between piles (cm)	Column section (cm×cm)	Column reinforcement rate (%)	θ (°)	$f_{c,exp}$ (MPa)
A-1	2	250	800	10×10	500	20×20	–	48.00	27.20
B-1	2	250	800	10×10	500	20×20	–	48.00	23.90
C-1	2	250	800	10×10	500	20×20	–	48.00	23.90

Note: all pile caps were 150 cm wide.

By balancing the forces in the x and y directions, the following equations are obtained:

$$R_{est} = \frac{F_{u,exp}}{n° \text{ of piles}} \tag{1}$$

$$R_{est} = R_{cc} \cdot \sin(\theta) \tag{2}$$

$$R_{st} = R_{cc} \cdot \cos(\theta) \tag{3}$$

in which:

$F_{u,exp}$ is the ultimate experimental force applied to the column;

R_{est} is the reaction of $F_{u,exp}$ on each pile;

R_{cc} is the resulting force on compressed concrete (resulting force on the strut);

R_{st} is the resulting force on the reinforcing steel (resulting force on the tie) and;

θ is the strut angle of inclination.

Equations [1] and [2] were used to determine the stress acting on the struts and on the nodes according to each one of the afore-mentioned models.
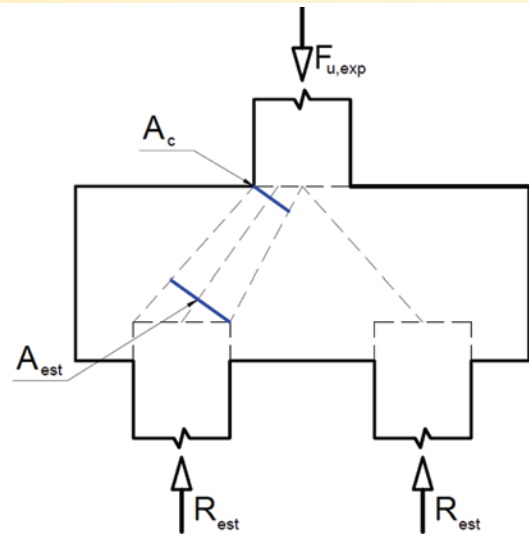

Figure 3
Pile area (A_{est}) and column area (A_c) both projected along the direction of the strut axis, adapted according to Blévot and Frémy [2]

Table 3
Properties of the pile caps analyzed by Adebar *et al.* [4]

Tested model	Pile number	Height (cm)	Length (cm)	Pile diameter (cm)	Distance between piles x (cm)	Distance between piles y (cm)	Column section (cm×cm)	Column reinforcement rate (%)	θ_x (°)	θ_x (°)	$f_{c,exp}$ (MPa)
A	4	60	–	20	156	90	30×30	0.891	37.57	53.13	24.80
B	4	60	–	20	156	90	30×30	0.891	37.57	53.13	24.80
C	6	60	260	20	90	90	30×30	0.891	30.81	53.13	27.10
D	4	60	–	20	156	90	30×30	0.891	37.57	53.13	30.30
E	4	60	–	20	156	90	30×30	0.891	37.57	53.13	41.10
F	4	60	–	20	156	90	30×30	0.891	37.57	53.13	30.30

Note: Pile cap C was a rectangular pile cap 170 cm wide, the other pile caps had hexagonal geometry according to Figure [1].

Table 4
Properties of the pile caps analyzed by Chan and Poh [7]

Tested model	Pile number	Height (cm)	Length (cm)	Pile section (cm×cm)	Distance between piles (cm)	Column section (cm×cm)	Column reinforcement rate (%)	θ (°)	$f_{c,exp}$ (MPa)
A	4	40	100	15×15	60	20×20	–	43.31	39.70
B	4	40	100	15×15	60	20×20	–	43.31	38.30
C	4	30	100	15×15	60	20×20	–	35.26	36.40

Note: all pile caps were 100 cm wide.

Table 5
Properties of the pile caps analyzed by Mautoni [5]

Tested model	Pile number	Height (cm)	Length (cm)	Pile section (cm×cm)	Distance between piles (cm)	Column section (cm×cm)	Column reinforcement rate (%)	θ (°)	$f_{c,exp}$ (MPa)
B20A1/1	3	60	–	20	96	35×35	9.816	52.00	27.40
B20A1/2	3	60	–	20	96	35×35	9.816	52.00	33.00
B20A2	3	60	–	20	96	35×35	9.816	52.00	35.50
B20A3	3	60	–	20	96	35×35	9.816	52.00	37.90
B20A4	3	60	–	20	96	35×35	9.816	52.00	35.60
B30A1	3	60	–	30	96	35×35	9.816	52.00	31.00
B30A2	3	60	–	30	96	35×35	9.816	52.00	40.30
B30A3	3	60	–	30	96	35×35	9.816	52.00	24.50
B30A4	3	60	–	30	96	35×35	9.816	52.00	24.60

2.1 Calculation of the acting stresses

Blévot and Frémy [2] present simple formulation for the calculation of the

nodal stresses. The model contemplates only the value of the force applied to the column, the column cross-sectional area and the pile cross-sectional area, both projected in the direction of the strut, see Figure [3].

Table 6
Properties of the pile caps analyzed by Delalibera and Giongo [9]

Tested model	Pile number	Height (cm)	Length (cm)	Pile section (cm×cm)	Distance between piles (cm)	Column section (cm×cm)	Column reinforcement rate (%)	θ (°)	$f_{c,exp}$ (MPa)
B35P25E25 and 0	2	35	117.50	25×25	62.50	25×25	1.0053	45.00	40.60
B35P25E25 and 2,5	2	35	117.50	25×25	62.50	25×25	1.0053	45.00	40.60
B35P25E25 and 0$_{AswC}$	2	35	117.50	25×25	62.50	25×25	1.0053	45.00	32.80
B35P25E25 and 0A$_{sw0}$	2	35	117.50	25×25	62.50	25×25	1.0053	45.00	32.80
B35P25E25 and 0CG	2	35	117.50	25×25	62.50	25×25	1.0053	45.00	28.90
B45P25E25 and 0	2	45	117.50	25×25	62.50	25×25	2.7489	54.50	31.00
B45P25E25 and 5	2	45	117.50	25×25	62.50	25×25	2.7489	54.50	31.00
B45P25E25 and 0A$_{swC}$	2	45	117.50	25×25	62.50	25×25	2.7489	54.50	32.40
B45P25E25 and 0A$_{sw0}$	2	45	117.50	25×25	62.50	25×25	2.7489	54.50	32.40
B45P25E25 and 0CG	2	45	117.50	25×25	62.50	25×25	2.7489	54.50	28.90
B35P50E25 and 0	2	35	117.50	25×25	62.50	25×50	0.87965	53.10	35.80
B35P50E25 and 12.5	2	35	117.50	25×25	62.50	25×50	0.87965	53.10	35.10
B45P50E25 and 0	2	45	117.50	25×25	62.50	25×50	1.3745	61.80	35.80
B45P50E25 and 12.5	2	45	117.50	25×25	62.50	25×50	1.3745	61.80	35.10

Note: the pile caps were 25 cm wide.

Table 7
Properties of the pile caps analyzed by Barros [10]

Tested model	Pile number	Height (cm)	Length (cm)	Pile section (cm×cm)	Distance between piles (cm)	Column section (cm×cm)	Column reinforcement rate (%)	θ (°)	$f_{c,exp}$ (MPa)
SR/M1	2	70	185	15×15	125	15×15	2.181	37.30	33.10
CR/M8	2	61	170	15×15	110	15×15	2.181	66.50	33.10

Note: the pile caps were 60 cm wide.

Table 8
Properties of the pile caps analyzed by Munhoz [11]

Tested model	Pile number	Height (cm)	Length (cm)	Pile section (cm×cm)	Distance between piles (cm)	Column section (cm×cm)	Column reinforcement rate (%)	θ (°)	$f_{c,exp}$ (MPa)
B110P125R1	2	40	110	12.5×12.5	60	12.5×12.5	5.12	56.30	30.47
B110P125R25	2	40	110	12.5×12.5	60	12.5×12.5	5.12	53.20	30.47
B110P125R4	2	40	110	12.5×12.5	60	12.5×12.5	5.12	43.90	30.47
B115P125R1	2	40	115	12.5×12.5	65	12.5×25	5.12	53.00	30.47
B115P125R25	2	40	115	12.5×12.5	65	12.5×25	5.12	49.30	30.47
B115P125R4	2	40	115	12.5×12.5	65	12.5×25	5.12	57.40	30.47
B120P125R1	2	40	120	12.5×12.5	70	12.5×37.5	4.267	55.70	30.47
B120P125R25	2	40	120	12.5×12.5	70	12.5×37.5	4.267	51.90	30.47
B120P125R4	2	40	120	12.5×12.5	70	12.5×37.5	4.267	55.20	30.47
B127P125R1	2	40	127	12.5×12.5	75	12.5×50	4.48	52.90	30.47
B127P125R25	2	40	127	12.5×12.5	75	12.5×50	4.48	49.60	30.47
B127P125R4	2	40	127	12.5×12.5	75	12.5×50	4.48	53.60	30.47

Note: the pile caps were 15 cm wide.

Table 9
Properties of the pile caps analyzed by Mesquita [12]

Tested model	Pile number	Height (cm)	Length (cm)	Pile section (cm×cm)	Distance between piles (cm)	Column section (cm×cm)	Column reinforcement rate (%)	θ (°)	$f_{c23,exp}$ (MPa)
M	2	30	100	20×20	50	20×20	8.043	56.31	42.21

Note: the pile caps were 50 cm wide; the $f_{c23,exp}$ value corresponds to the concrete strength at 23 days.

Table 10
Properties of the pile caps analyzed by Cao and Bloodworth [13]

Tested model	Pile number	Height (cm)	Length (cm)	Pile section (cm×cm)	Distance between piles (cm)	Column section (cm×cm)	Column reinforcement rate (%)	θ (°)	$f_{c,exp}$ (MPa)
B4A1	4	23	110	13	80	20×50	–	24.98	20.30
B4A2	4	23	95	13	65	20×50	–	29.07	21.80
B4A3	4	23	85	13	55	20×50	–	32.43	24.30
B4A4	4	23	80	13	50	20×50	–	34.32	24.40
B4A5	4	23	70	13	40	20×50	–	38.52	23.00
B4B2	4	23	95	13	65	20×65	–	26.84	25.60
B4B3	4	23	95	13	65	20×75	–	25.16	24.70

Note: the first 5 models were 50 cm wide, the others were 65 cm and 75 cm wide, respectively.

The upper nodal stress (contact stress between column/pile cap) is calculated by equation [4], while the nodal stress for the lower nodal zone (contact stress between pile cap/pile) are calculated by equations [5], [6] and [7] for caps on two, three and four piles, respectively.

$$\sigma_{zns} = \frac{F_{u,exp}}{A_c \cdot \sin^2(\theta)} \tag{4}$$

$$\sigma_{zni} = \frac{F_{u,exp}}{2 \cdot A_{est} \cdot \sin^2(\theta)} \tag{5}$$

$$\sigma_{zni} = \frac{F_{u,exp}}{3 \cdot A_{est} \cdot \sin^2(\theta)} \tag{6}$$

$$\sigma_{zni} = \frac{F_{u,exp}}{4 \cdot A_{est} \cdot \sin^2(\theta)} \tag{7}$$

in which:
$F_{u,exp}$, is the ultimate experimental force applied to the column;
A_c is the column cross-sectional area;
A_{est} is the pile cross-sectional area and;
θ is the strut angle of inclination.
Schlaich and Schäfer [14] proposed a more precise formulation, in which they consider the type of truss node. The authors differentiate existing nodes according to the acting stress and the presence or not of anchored bars. In this way, the upper nodal region is represented by Figure [4], node only subjected to compressive stresses, and the lower nodal region is represented by Figure [5], node where the bars are anchored, therefore, with incidence of tensile stresses.
The analysis of Figure [4] suggests that the upper node is subject-

ed to the triple stress state, since the volume of delimited concrete by a_0 is subjected to compressive forces acting in different directions. According to Schlaich and Schäfer [14], it is convenient to choose the a_0 value as presented by equation [8].

$$a_0 \geq a_1 \cdot \cos(\theta_2) \cdot \sin(\theta_2) = a_1 \cdot \cos(\theta_3) \cdot \sin(\theta_3) \tag{8}$$

However, a limit value for a_0 is not presented. The upper and lower nodal stresses calculation is done using equations [9] and [10] respectively.

$$\sigma_{zns} = \frac{F_{u,exp}}{a_1 \cdot b} \tag{9}$$

$$\sigma_{zni} = \frac{R_{est}/A_{est}}{\left[1 + \left(\frac{u \cdot \cot g(\theta)}{a_1}\right)\right] \cdot \sin^2(\theta)} \tag{10}$$

being that:
$F_{u,exp}$, is the ultimate experimental force applied to the column;
R_{est} is the reaction of $F_{u,exp}$ on each pile;
A_{est} is the pile cross-sectional area;
a_0 is the area of contribution near the upper nodal zone;
a_1 is the dimension of column or pile, measured in the direction of the strut;
b is the dimension of the column measured in a direction perpendicular to the strut;
u is the height in which longitudinal rebar is distributed considering a top concrete cover layer and;
θ is the strut angle of inclination.
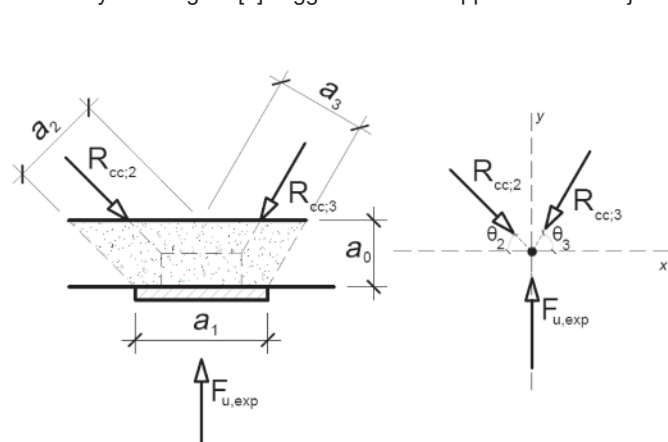

Figure 4
Node subjected only to compressive stresses, adapted according to Schlaich and Schäfer [14]
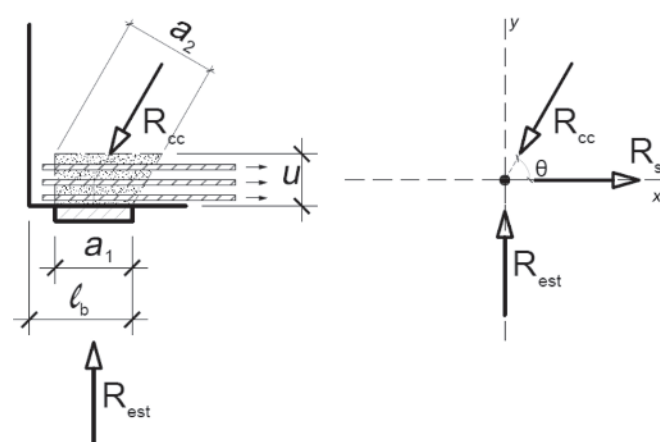

Figure 5
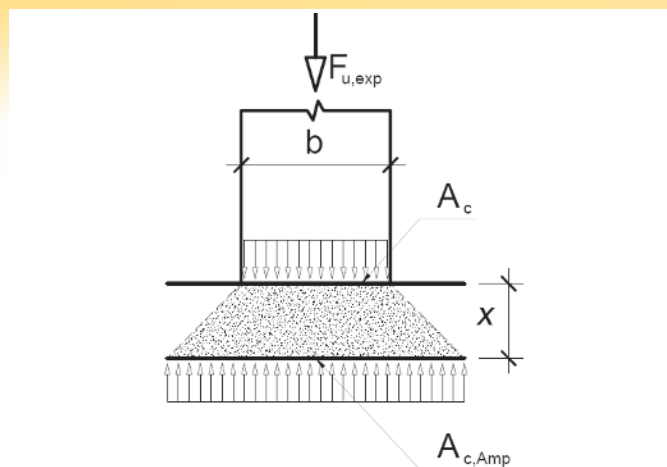Node with anchored bars, adapted according to Schlaich and Schäfer [14]

Figure 6
Extended area $A_{c,Amp}$, adapted according
to Fusco [15]

Unlike the other authors, Fusco [15] suggests that the column re-inforcement rate affects the transmission of the compressive force from the colum to the pile cap.

As shown in Figure [6], Fusco [15] analyzes the compressive stress in an amplified concrete area $A_{c,Amp}$, at an x value of distance from the top of the pile cap.

This enlarged area is approximately nine times larger than the column section area and its position depends only on the column's re-inforcement rate. As shown in Table [21], the higher the reinforcement rate existing in the column, the furthest from the upper face is the area $A_{c,Amp}$. The value of x is only indicative of the position of the enlarged area in relation to the upper face of the pile cap, since the position of x does not interfere with the value of $A_{c,Amp}$.

Another important aspect is that Fusco [15] indicates that the stress in the lower nodal zone is within acceptable limits based on the stress acting on the pile. So, according to the model proposed by Fusco [15], it is possible to calculate the stresses in the upper nodal zones and lower with equations [11] and [12], respectively.

$$\sigma_{zns} = \frac{\sigma_{cv,d}}{\sin^2(\theta)} \tag{11}$$

$$\sigma_{zni} = \frac{R_{est}}{1,4 \cdot A_{est}} \tag{12}$$

being that:
$\sigma_{cv;d}$ is the vertical stress at the x depth from the top of the cap,

calculated by $\frac{F_{u,exp}}{A_{c,Amp}}$;

$F_{u,exp}$ is the the ultimate load applied to the column;
$A_{c,Amp}$ is the cross-sectional area of the column pivoted at x depth relative to the top of the pile cap;
R_{est} is the reaction on the pile;
A_{est} is the pile cross-sectional area and;
θ is the strut angle of inclination.

2.2 Limits of nodal stress values

As the purpose of this work is to compare the stresses calculation models with the limits indicated by the norms, the limits proposed by the authors Blévot and Frémy [2], Schlaich and Schäfer [14] and Fusco [15], as well as the norms ABNT NBR 6118:2014 [3], EHE-1998 [16], ACI 318-14 [17], CEB-*fib* [18] and CEB-*fib* [19] were considered.

As for the experimental data, the coefficient γ_c that lowers the resistance of the concrete was not considered, as it is used only for design. In the same way, the Rüsch effect and the α_{v2} coefficient were not considered, since the forces applied in the models up to their failure were not of long duration.

Table [22] shows all the limits considered for the analysis according to the following types of nodes:

■ Node CCC – prismatics strut;
■ Node CCT – struts crossed by a single tie and;
■ Node CTT ou TTT – struts crossed by more than one tie.

Considering that the concrete in the column/cap contact region subjected to a triple stress state, it is proposed by the authors of this work that the stress limit for the upper nodal zone is equal to the concrete strength on triple stress state proposed in ABNT NBR 6118:2014 [3]. If the concrete is subjected to the triple stress state, considering $\sigma_3 \geq \sigma_2 \geq \sigma_1$, the following limit is considered:

$$\sigma_3 = f_{ck} + 4 \cdot \sigma_1 \tag{13}$$

being that: $\sigma_1 \geq -f_{ctk}$ (being the tensile stress considered negative). In this way, the limit value for the stress in the upper nodal zone is a value higher than the proposed value (for CCC nodes) by ABNT NBR 6118:2014 [3].

Finally, the authors make an observation regarding the limits presented. The book ABNT NBR 6118: 2014 *Comentários e Exemplos de Aplicação* [20], edited by the Instituto Brasileiro do Concreto (IBRACON), is mistaken about the limits established by Blévot and Frémy [2]. In the publication it is said that the limits for nodal stresses, both upper and lower, depend on an α factor, and that such factor depends on the number of piles in which the pile cap is supported. The book considers that the α value is applied to both the upper nodal zone and the lower nodal zone.

According to Blévot and Frémy [2], the value of α should be applied only to the upper nodal zone, as shown in Table [22].

3. Results and discussions

For each pile cap tested from each of the mentioned authors, the ultimate experimental force and the angle of inclination of the struts were extracted. With this information, equations [1], [2] and [3] were applied to find reaction forces on piles, on the struts and on the ties that acted on the models. The results of this calculation step are shown in Tables [11] to [20].

Thus, with such forces, it is possible to apply the models for calculating the nodal stresses and compare with each of the limits presented by Table [22].

Looking closely at Table [22] it is noted that, after excluding the safety coefficients, many limits became equal. Thus, it can be verified that one of the factors that cause the discrepancy between the limits are the safety coefficients that each norm and authors adopt.

The obtained results for the operating stresses and limit stresses for the last test situation for both the upper nodal zone (σ_{zns}) and the lower nodal zone (σ_{zni}) of each author, according to the presented equations, are shown in Tables [23] to [33].

In order to facilitate the understanding, the graphs of Figures [7] to [26] show, for each author, on the x-axis the tested model and on the y-axis the values of the stresses calculated by each of the aforementioned methods. The horizontal lines represent the mean values of the limiting stresses in kN/cm². Figures [27] and [28] show all models in a single graph.

The analysis of the graphs confirms the discrepancy between the limits, however, the boundaries for the lower nodal zone are closer than the upper nodal zone limits for all pile caps.

For the caps tested by Mautoni [5], it is observed that the limits

established by Schlaich and Schäfer [14] and CEB-*fib* [19] for the lower nodal zone show values closer to the mean value, whereas for the upper nodal zone, the stresses are better represented by both the Schlaich and Schäfer limits [19] and by the limits of CEB-*fib* [19] and ACI 318-14 [17].

The same reasoning can be expanded to the other cases, except for the caps tested by Adebar et al. [4]. The fact of laying the piles

in different distances in x and y, generated considerable variations in the calculated stresses.

The consideration of the multiaxial state of stresses was shown to be coherent in all cases, being the calculated value close to the value established by Schlaich and Schäfer [14].

In some particular cases, such as Chan and Poh [7] and Mesquita [12], the stresses for the lower nodal zone calculated by the Fusco [15]

Table 11
Forces acting in the tests performed by Mautoni [5]

Tested model	F_r (kN)	$F_{u,exp}$ (kN)	R_{est} (kN)	R_{cc} (kN)	R_{st} (kN)
B1-1	368,669	508,165	254,083	306,394	171,230
B2-1	318,849	508,165	254,083	306,394	171,230
B1-2	199,280	348,741	174,371	212,412	121,301
B2-2	199,280	348,741	174,371	212,412	121,301
B1-A	348,741	474,301	237,151	288,889	164,974
B2-A	348,741	747,301	373,651	455,169	259,931
B1-B	348,741	727,373	363,687	465,746	290,949
B2-B	318,849	727,373	363,687	465,746	290,949
B1-4A	298,920	667,589	333,795	427,466	267,036
B2-4A	318,849	667,589	333,795	427,466	267,036
B1-4B	308,884	627,733	313,867	401,945	251,093
B2-4B	318,849	627,733	313,867	401,945	251,093
B1-4C	249,100	498,201	249,101	319,004	199,280
B2-4C	298,920	498,201	249,101	319,004	199,280
D1	229,172	508,165	254,083	330,741	211,735
D2	229,172	508,165	254,083	330,741	211,735
F1	229,172	478,723	239,362	338,508	239,362
F2	209,244	478,273	239,137	338,190	239,137
E1	169,388	368,669	184,335	277,460	207,376
G1	199,280	458,345	229,173	344,950	257,819

Table 12
Forces acting in the tests performed by Fusco [6]

Tested model	F_r (kN)	$F_{u,exp}$ (kN)	R_{est} (kN)	R_{cc} (kN)	R_{st} (kN)
A-1	–	393.000	196.500	264.417	176.929
B-1	150.000	400.000	200.000	269.127	180.081
C-1	150.000	400.000	200.000	269.127	180.081

Table 13
Forces acting in the tests performed by Adebar *et al.* [4]

Tested model	F_r (kN)	$F_{u,exp}$ (kN)	$R_{est;x}$ (kN)	$R_{est;y}$ (kN)	$R_{cc;x}$ (kN)	$R_{cc;y}$ (kN)	$R_{st;x}$ (kN)	$R_{st;y}$ (kN)
A	–	1,781.000	445.250	445.250	730.264	556.563	578.825	333.938
B	–	2,189.000	547.250	547.250	897.557	684.063	711.425	410.438
C	–	2,892.000	723.000	723.000	1,411.702	1,411.702	1,212.507	1,212.507
D	–	3,222.000	805.500	805.500	1,321.118	1,006.875	1,407.150	604.125
E	–	4,709.000	1,177.250	1,177.250	1,930.833	1,471.563	1,530.425	882.938
F	–	3,026.000	756.500	756.500	1,240.752	945.625	983.450	567.375

Table 14
Forces acting in the tests performed by Chan and Poh [7]

Tested model	F_r (kN)	$F_{u,exp}$ (kN)	R_{est} (kN)	R_{cc} (kN)	R_{st} (kN)
A	840.000	1.230.000	307.500	448.286	326.197
B	900.000	1.250.000	312.500	455.576	331.501
C	450.000	870.000	217.500	376.762	307.641

Table 15
Forces acting in the tests performed by Miguel [8]

Tested model	F_r (kN)	$F_{u,exp}$ (kN)	R_{est} (kN)	R_{cc} (kN)	R_{st} (kN)
B20A1/1	1,050.000	1,512.000	504.000	639.858	393.768
B20A1/2	900.000	1,648.000	549.334	697.114	429.186
B20A2	1,050.000	2,083.000	694.334	881.122	542.473
B20A3	1,050.000	1,945.000	648.334	822.747	506.534
B20A4	1,200.000	2.375.000	791.667	1,004.639	618.518
B30A1	900.000	1,909.000	636.334	807.519	497.158
B30A2	1,050.000	2,674.000	891.334	1,131.118	696.386
B30A3	750.000	1,938.000	646.000	819.786	504.711
B30A4	900.000	2,283.000	761.000	965.723	594.558

Table 16
Forces acting in the tests performed by Delalibera and Giongo [9]

Tested model	F_r (kN)	$F_{u,exp}$ (kN)	R_{est} (kN)	R_{cc} (kN)	R_{st} (kN)
B35P25E25 and 0	465.000	1,821.000	910.500	1,287.641	910.500
B35P25E25 and 2.5	445.000	1,688.000	844.000	1,193.596	844.000
B35P25E25 and $0A_{swC}$	270.000	1,880.000	940.000	1,329.361	940.000
B35P25E25 and $0A_{sw0}$	266.000	1,406.000	703.000	994.192	703.000
B35P25E25 and 0CG	315.000	1,263.000	631.500	893.076	631.500
B45P25E25 and 0	465.000	2,276.000	1,138.000	1,397.836	811.728
B45P25E25 and 5	522.000	1,972.000	986.000	1,211.130	703.307
B45P25E25 and $0A_{swC}$	482.000	3,055.000	1,527.500	1,879.269	1,089.555
B45P25E25 and $0A_{sw0}$	305.000	2,090.000	1,045.000	1,283.602	745.391
B45P25E25 and 0CG	473.000	2,270.000	1,135.000	1,394.151	809.588
B35P50E25 and 0	450.000	3,877.000	1,938.500	2,424.081	1,455.467
B35P50E25 and 12.5	585.000	3,202.000	1,601.000	2,002.039	1,202.065
B45P50E25 and 0	851.000	4,175.000	2,087.500	2,368.651	1,119.308
B45P50E25 and 12.5	477.000	3,386.000	1,693.000	1,921.018	907.779

Table 17
Forces acting in the tests performed by Barros [10]

Tested model	F_r (kN)	$F_{u,exp}$ (kN)	R_{est} (kN)	R_{cc} (kN)	R_{st} (kN)
SR/M1	210.000	756.750	378.000	409.739	158.121
CR/M8	200.000	725.000	362.500	395.285	157.619

Table 18
Forces acting in the tests performed by Munhoz [11]

Tested model	F_r (kN)	$F_{u,exp}$ (kN)	R_{est} (kN)	R_{cc} (kN)	R_{st} (kN)
B110P125R1	225.000	431.110	215.555	259.095	143.757
B110P125R25	198.000	577.080	288.540	360.346	215.855
B110P125R4	240.000	590.730	295.365	425.965	306.930
B115P125R1	158.000	712.670	356.335	446.180	268.518
B115P125R25	148.000	736.020	368.010	485.415	316.539
B115P125R4	154.000	763.640	381.820	453.224	244.184
B120P125R1	235.000	850.780	425.390	514.939	290.181
B120P125R25	198.000	807.130	403.656	512.831	316.435
B120P125R4	201.000	924.260	462.130	562.784	321.189
B127P125R1	276.000	1.028.300	514.150	644.634	388.849
B127P125R25	247.000	979.880	489.940	643.356	416.972
B127P125R4	185.000	969.350	484.675	602.160	357.333

Table 19
Forces acting in the tests performed by Mesquita [12]

Tested model	F_r (kN)	$F_{u,exp}$ (kN)	R_{est} (kN)	R_{cc} (kN)	R_{st} (kN)
M	600.000	2,150.000	1,075.000	1,291.988	716.665

Table 20
Forces acting in the tests performed by Cao and Bloodworth [13]

Tested model	F_r (kN)	$F_{u,exp}$ (kN)	R_{est} (kN)	R_{cc} (kN)	R_{st} (kN)
B4A1	–	592.000	148.000	350.497	317.717
B4A2	–	548.000	137.000	281.947	246.425
B4A3	–	919.000	229.750	428.460	361.653
B4A4	–	1,052.000	263.000	466.512	385.311
B4A5	–	1,244.000	311.000	499.370	390.703
B4B2	–	713.000	178.250	394.825	352.297
B4B3	–	769.000	192.250	452.146	409.238

model are far below the limit values, including the limit values stipulated by Fusco [15].

For the models tested by Delalibera and Giongo [9] whose name ends with $A_{sw,C}$, the acting stresses were slightly higher because these models were detailed with a reinforcement designed to absorb the stresses that cause cracking of the compression struts. There was also a variability in the stresses when an eccentricity in the applied force was considered, as can be observed in models ending with e0, e2,5, e5 and e12,5.

The values of stresses calculated by the three proposed methods were conflicting with each other. The fact that Fusco [15] considered the stress in the upper nodal zone calculated in an area $A_{c,Amp}$ made the values much smaller in relation to the other calculated values. This fact is reflected in the limits, the model of calculation of stresses proposed by Fusco [15] is compatible only with the limits established by himself, however, it is necessary to point out that it is not clear how the author found the proposed limits.

The stresses calculated by the method of Schlaich and Schäfer [14] are those that present better results, since the values do not show great variability, which did not occur with the values calculated by the Blévot and Frémy [2] model. The stresses calculated by Blévot and Frémy [2] are, in many cases, outside the presented limits.

4. Conclusions

Analyzing the presented formulations for the calculation of stresses and limit values, the discrepancy between each method is evident. Therefore, the same pile cap can be considered "verified" or not depending on the model used to analyze the stresses.

The mean limit values for the lower nodal zone are closer to the mean values for the upper nodal zone, showing that the greatest

Table 21
x/b values according to Fusco [15]

Column reinforcement rate (%)	1%	2%	3%
Square columns	0.8	1.0	1.2
Very wide columns	0.35	0.42	1.0

Note: b is the smallest plan dimension of the column.

discrepancy between the limits lies in the upper nodal zone.

Consideration of the multiaxial stress state of the concrete leads to intermediate values in relation to the values presented by Blévot and Frémy [2] and by Schlaich and Schäfer [14], which are higher than those indicated by ABNT NBR 6118:2014 [3], with the limit value that considers the multiaxial stress state being more representative when compared to the ultimate stress of the upper nodal zone.

The model presented by Fusco [15] discusses considerations regarding the upper nodal area that are not very clear, since there is no precise demonstration for the limit value of 2/9 f_c. The consideration of an amplified area $A_{c,Amp}$, distant x from the upper face of the pile cap, causes the stresses to be very different when compared with the other methods. The stresses calculated by the Fusco [15] method are compatible only with the limit values presented by himself, therefore, the limits described by ABNT NBR 6118:2014 [3] cannot be applied when the stresses are calculated using the Fusco [15] model.

The limit given by the Spanish standard EHE-1998 [16] for the upper nodal zone is much higher than the other limits, as well as much higher than the value of the calculated stresses, so caution is recommended when considering it, because the analyzed pile caps failed with values of stress in the upper nodal zone

Table 22
FLimit values of stress for nodal regions without considering γ_c, the Rüsch effect and α_{v2}

Criteria	CCC	CCT	CTT or TTT
Blévot and Frémy [2]		1.40 f_c; upper nodal area (for pile caps on two piles) 1.75 f_c; upper nodal area (for pile caps on three piles) 2.10 f_c; upper nodal area (for pile caps on four piles) f_c; lower nodal zone (for pile caps in any situation)	
Schlaich and Schäfer [14]	1.10 f_c	0.80 f_c	0.80 f_c
Fusco [15]	2/9 f_c	0.50 f_c	0.50 f_c
ABNT NBR 6118:2014 [2]	0.85 f_c	0.72 f_c	0.60 ff$_c$
EHE-1998 [16]	3.00 f_c	0.70 f_c	0.70 f_c
ACI-2014 [17]	0.85 f_c	0.68 f_c	0.51 f_c
CEB-fib [18]	0.85 f_c	0.60 f_c	0.60 f_c
CEB-fib [19]	1.00 f_c	0.75 f_c	0.75 f_c
Triple stress state	$f_{ck} + 4 f_{ctk}$	–	–

Table 23
Active stresses × Limits considered for Mautoni's [5] tests

	Active stresses (kN/cm²)					
Tested model	Blévot and Frémy [2]		Fusco [15]		Schlaich and Schäfer [14]	
	σ_{zni}	σ_{zns}	σ_{zni}	σ_{zns}	σ_{zni}	σ_{zns}
B1-1	2.46	3.28	1.21	0.36	1.55	2.26
B2-1	2.46	3.28	1.21	0.36	1.55	2.26
B1-2	1.73	2.30	0.83	0.26	1.07	1.55
B2-2	1.73	2.30	0.83	0.26	1.07	1.55
B1-A	2.35	3.13	1.13	0.35	1.46	2.11
B2-A	3.70	4.93	1.78	0.55	2.30	3.32
B1-B	3.98	5.30	1.73	0.59	2.34	3.23
B2-B	3.98	5.30	1.73	0.59	2.34	3.23
B1-4A	3.65	4.87	1.59	0.54	2.15	2.97
B2-4A	3.65	4.87	1.59	0.54	2.15	2.97
B1-4B	3.43	4.58	1.49	0.51	2.02	2.79
B2-4B	3.43	4.58	1.49	0.51	2.02	2.79
B1-4C	2.72	3.63	1.19	0.40	1.60	2.21
B2-4C	2.72	3.63	1.19	0.40	1.60	2.21
D1	2.87	3.83	1.21	0.43	1.66	2.26
D2	2.87	3.83	1.21	0.43	1.66	2.26
F1	3.19	4.26	1.14	0.47	1.70	2.13
F2	3.19	4.25	1.14	0.47	1.70	2.13
E1	2.78	3.71	0.88	0.41	1.40	1.64
G1	3.46	4.62	1.09	0.51	1.74	2.04

Limit stresses (kN/cm²)																
Blévot and Frémy [2]		Fusco [15]		Schlaich and Schäfer [14]		ABNT NBR 6118:2014 [2]		EHE-1998 [16]		ACI 318-14 [17]		CEB-*fib* 1990 [18]		CEB-*fib* 2010 [19]		Triple stress state
σ_{zni}	σ_{zns}	σ_{zni}	σ_{zns}	σ_{zni}	σ_{zns}	σ_{zni}	σ_{zns}	σ_{zni}	σ_{zns}	σ_{zni}	σ_{zns}	σ_{zni}	σ_{zns}	σ_{zni}	σ_{zns}	σ_{zns}
2.15	3.01	1.08	1.48	1.72	2.37	1.55	1.83	1.51	6.45	1.72	2.15	1.29	1.83	1.61	2.15	3.08
2.15	3.01	1.08	0.48	1.72	2.37	1.55	1.83	1.51	6.45	1.72	2.15	1.29	1.83	1.61	2.15	3.08
1.50	2.10	0.75	0.33	1.20	1.65	1.08	1.28	1.05	4.50	1.20	1.50	0.90	1.28	1.13	1.50	2.23
1.50	2.10	0.75	0.33	1.20	1.65	1.08	1.28	1.05	4.50	1.20	1.50	0.90	1.28	1.13	1.50	2.23
3.23	4.42	1.62	0.72	2.58	3.55	2.33	2.75	2.26	9.69	2.58	3.23	1.94	2.75	2.42	3.23	4.45
3.23	4.52	1.62	0.72	2.58	3.55	2.33	2.75	2.26	9.69	2.58	3.23	1.94	2.75	2.42	3.23	4.45
3.20	4.48	1.60	0.71	2.56	3.52	2.30	2.72	2.24	9.60	2.56	3.20	1.92	2.72	2.40	3.20	4.41
3.20	4.48	1.60	0.71	2.56	3.52	2.30	2.72	2.24	9.60	2.56	3.20	1.92	2.72	2.40	3.20	4.41
2.95	4.13	1.48	0.66	2.36	3.25	2.12	2.51	2.07	8.85	2.36	2.95	1.77	2.51	2.21	2.95	4.10
2.95	4.13	1.48	0.66	2.36	3.25	2.12	2.51	2.07	8.85	2.36	2.95	1.77	2.51	2.21	2.95	4.10
2.78	3.89	1.39	0.62	2.22	3.06	2.00	2.36	1.95	8.34	2.22	2.78	1.67	2.36	2.09	2.78	3.88
2.78	3.89	1.39	0.62	2.22	3.06	2.00	2.36	1.95	8.34	2.22	2.78	1.67	2.36	2.09	2.78	3.88
2.22	3.11	1.11	0.49	1.78	2.44	1.60	1.89	1.55	6.66	1.78	2.22	1.33	1.89	1.67	2.22	3.17
2.22	3.11	1.11	0.49	1.78	2.44	1.60	1.89	1.55	6.66	1.78	2.22	1.33	1.89	1.67	2.22	3.17
2.29	3.21	1.15	0.51	1.83	2.52	1.65	1.95	1.60	6.87	1.83	2.29	1.37	1.95	1.72	2.29	3.26
2.29	3.21	1.15	0.51	1.83	2.52	1.65	1.95	1.60	6.87	1.83	2.29	1.37	1.95	1.72	2.36	3.26
2.36	3.30	1.18	0.52	1.89	2.60	1.70	2.01	1.65	7.08	1.89	2.36	1.42	2.01	1.77	2.36	3.35
2.36	3.30	1.18	0.52	1.89	2.60	1.70	2.01	1.65	7.08	1.89	2.36	1.42	2.01	1.77	2.36	3.35
1.95	2.73	0.98	0.43	1.56	2.15	1.40	1.66	1.37	5.85	1.56	1.95	1.17	1.66	1.46	1.95	2.82
2.43	3.40	1.22	0.54	1.94	2.67	1.75	2.07	1.70	7.29	1.94	2.43	1.46	2.07	1.82	2.43	3.44
Limit stresses average																
2.49	3.48	1.24	0.55	1.99	2.74	1.79	2.11	1.74	7.46	1.99	2.49	1.49	2.11	1.87	2.49	3.50

Table 24
Active stresses × Limits considered for Fusco's [6] tests

	Active stresses (kN/cm²)					
Tested model	**Blévot and Frémy [2]**		**Fusco [15]**		**Schlaich and Schäfer [14]**	
	σ_{zni}	σ_{zns}	σ_{zni}	σ_{zns}	σ_{zni}	σ_{zns}
A-1	3.56	1.78	1.40	0.20	2.89	0.98
B-1	3.62	1.81	1.43	0.20	2.95	1.00
C-1	3.62	1.81	1.43	0.20	2.95	1.00

Limit stresses (kN/cm²)																
Blévot and Frémy [2]		**Fusco [15]**		**Schlaich and Schäfer [14]**		**ABNT NBR 6118:2014 [2]**		**EHE-1998 [16]**		**ACI 318-14 [17]**		**CEB-*fib* 1990 [18]**		**CEB-*fib* 2010 [19]**		**Triple stress state**
σ_{zni}	σ_{zns}	σ_{zni}	σ_{zns}	σ_{zni}	σ_{zns}	σ_{zni}	σ_{zns}	σ_{zni}	σ_{zns}	σ_{zni}	σ_{zns}	σ_{zni}	σ_{zns}	σ_{zni}	σ_{zns}	σ_{zns}
2.72	3.81	1.36	0.60	2.18	2.99	1.96	2.31	1.90	8.16	2.18	2.72	1.63	2.31	2.04	2.72	3.81
2.39	3.35	1.20	0.53	1.91	2.63	1.72	2.03	1.67	7.17	1.91	2.39	1.43	2.03	1.79	2.39	3.39
2.39	3.35	1.20	0.53	1.91	2.63	1.72	2.03	1.67	7.17	1.91	2.39	1.43	2.03	1.79	2.39	3.39
Limit stresses average																
2.50	3.50	1.25	0.56	2.00	2.75	1.80	2.13	1.75	7.50	2.00	2.50	1.50	2.13	1.88	2.50	3.53

Table 25
Active stresses in x direction × Limits considered for Adebar et al. [4] tests

	Active stresses (kN/cm²)					
Tested model	**Blévot and Frémy [2]**		**Fusco [15]**		**Schlaich and Schäfer [14]**	
	σ_{zni}	σ_{zns}	σ_{zni}	σ_{zns}	σ_{zni}	σ_{zns}
A_x	3.81	5.32	1.01	0.59	3.81	1.98
B_x	4.69	6.54	1.24	0.73	2.37	2.43
C_x	8.77	12.25	1.64	1.36	7.51	3.21
D_x	6.90	9.63	1.83	1.07	3.49	3.58
E_x	10.08	14.07	2.68	1.56	8.92	5.23
F_x	6.48	9.04	1.72	1.00	3.28	3.36

Limit stresses (kN/cm²)																
Blévot and Frémy [2]		**Fusco [15]**		**Schlaich and Schäfer [14]**		**ABNT NBR 6118:2014 [2]**		**EHE-1998 [16]**		**ACI 318-14 [17]**		**CEB-*fib* 1990 [18]**		**CEB-*fib* 2010 [19]**		**Triple stress state**
σ_{zni}	σ_{zns}	σ_{zni}	σ_{zns}	σ_{zni}	σ_{zns}	σ_{zni}	σ_{zns}	σ_{zni}	σ_{zns}	σ_{zni}	σ_{zns}	σ_{zni}	σ_{zns}	σ_{zni}	σ_{zns}	σ_{zns}
2.48	5.21	1.24	0.55	1.98	2.73	1.49	2.11	1.74	7.44	1.49	2.48	1.49	2.11	1.86	2.48	3.50
2.48	5.21	1.24	0.55	1.98	2.73	1.49	2.11	1.74	7.44	1.49	2.48	1.49	2.11	1.86	2.48	3.50
2.71	5.69	1.36	0.60	2.17	2.98	1.63	2.30	1.90	8.13	1.63	2.71	1.63	2.30	2.03	2.71	3.79
3.03	6.36	1.52	0.67	2.42	3.33	1.82	2.58	2.12	9.09	1.82	3.03	1.82	2.58	2.27	3.03	4.20
4.11	8.63	2.06	0.91	3.29	4.52	2.47	3.49	2.88	12.33	2.47	4.11	2.47	3.49	3.08	4.11	5.54
3.03	6.36	1.52	0.67	2.42	3.33	1.82	2.58	2.12	9.09	1.82	3.03	1.82	2.58	2.27	3.03	4.20
Limit stresses average																
2.97	6.24	1.49	0.66	2.38	3.27	1.78	2.53	2.08	8.92	1.78	2.97	1.78	2.53	2.23	2.97	4.12

Table 26
Active stresses in y direction × Limits considered for Adebar *et al.* [4]

Tested model	Active stresses (kN/cm²)					
	Blévot and Frémy [2]		Fusco [15]		Schlaich and Schäfer [14]	
	σ_{zni}	σ_{zns}	σ_{zni}	σ_{zns}	σ_{zni}	σ_{zns}
A_y	2.21	3.09	1.01	0.34	2.06	1.98
B_y	2.72	3.80	1.24	0.42	1.74	2.43
C_y	8.77	12.25	1.64	1.36	7.51	3.21
D_y	4.01	5.59	1.83	0.62	2.56	3.58
E_y	5.86	8.18	2.68	0.91	5.45	5.23
F_y	3.76	5.25	1.72	0.58	2.41	3.36

Limit stresses (kN/cm²)																
Blévot and Frémy [2]		Fusco [15]		Schlaich and Schäfer [14]		ABNT NBR 6118:2014 [2]		EHE-1998 [16]		ACI 318-14 [17]		CEB-*fib* 1990 [18]		CEB-*fib* 2010 [19]		Triple stress state
σ_{zni}	σ_{zns}	σ_{zni}	σ_{zns}	σ_{zni}	σ_{zns}	σ_{zni}	σ_{zns}	σ_{zni}	σ_{zns}	σ_{zni}	σ_{zns}	σ_{zni}	σ_{zns}	σ_{zni}	σ_{zns}	σ_{zns}
2.48	5.21	1.24	0.55	1.98	3.50	1.49	2.11	1.74	7.44	1.49	2.48	1.49	2.11	1.86	2.48	3.50
2.48	5.21	1.24	0.55	1.98	3.50	1.49	2.11	1.74	7.44	1.49	2.48	1.49	2.11	1.86	2.48	3.50
2.71	5.69	1.36	0.60	2.17	3.79	1.63	2.30	1.90	8.13	1.63	2.71	1.63	2.30	2.03	2.71	3.79
3.03	6.36	1.52	0.67	2.42	4.20	1.82	2.58	2.12	9.09	1.82	3.03	1.82	2.58	2.27	3.03	4.20
4.11	8.63	2.06	0.91	3.29	5.54	2.47	3.49	2.88	12.33	2.47	4.11	2.47	3.49	3.08	4.11	5.54
3.03	6.36	1.52	0.67	2.42	4.20	1.82	2.58	2.12	9.09	1.82	3.03	1.82	2.58	2.27	3.03	4.20
Limit stresses average																
2.97	6.24	1.49	0.66	2.38	3.27	1.78	2.53	2.08	8.92	1.78	4.12	1.78	2.53	2.23	2.97	4.12

Table 27
Active stresses × Limits considered for Chan and Poh's [7] tests

Tested model	Active stresses (kN/cm²)					
	Blévot and Frémy [2]		Fusco [15]		Schlaich and Schäfer [14]	
	σ_{zni}	σ_{zns}	σ_{zni}	σ_{zns}	σ_{zni}	σ_{zns}
A	2.90	6.54	0.98	0.73	2.53	3.08
B	2.95	6.64	0.99	0.74	2.57	3.13
C	2.90	6.53	0.69	0.73	2.42	2.18

Limit stresses (kN/cm²)																
Blévot and Frémy [2]		Fusco [15]		Schlaich and Schäfer [14]		ABNT NBR 6118:2014 [2]		EHE-1998 [16]		ACI 318-14 [17]		CEB-*fib* 1990 [18]		CEB-*fib* 2010 [19]		Triple stress state
σ_{zni}	σ_{zns}	σ_{zni}	σ_{zns}	σ_{zni}	σ_{zns}	σ_{zni}	σ_{zns}	σ_{zni}	σ_{zns}	σ_{zni}	σ_{zns}	σ_{zni}	σ_{zns}	σ_{zni}	σ_{zns}	σ_{zns}
3.97	8.34	1.99	0.88	3.18	4.37	2.38	3.37	2.78	11.91	2.38	3.97	2.38	3.37	2.98	3.97	5.37
3.83	8.04	1.92	0.85	3.06	4.21	2.30	3.26	2.68	11.49	2.30	3.83	2.30	3.26	2.87	3.83	5.19
3.64	7.64	1.82	0.81	2.91	4.00	2.18	3.09	2.55	10.92	2.18	3.64	2.18	3.09	2.73	3.65	4.96
Limit stresses average																
3.81	8.01	1.91	0.85	3.05	4.19	2.29	3.24	2.67	11.44	2.29	3.81	2.29	3.24	2.86	3.81	5.17

Table 28
Active stresses × Limits considered for Miguel's [8] tests

Tested model	Active stresses (kN/cm²)					
	Blévot and Frémy [2]		Fusco [15]		Schlaich and Schäfer [14]	
	σ_{zni}	σ_{zns}	σ_{zni}	σ_{zns}	σ_{zni}	σ_{zns}
B20A1/1	2.58	1.99	1.15	0.22	2.29	1.23
B20A1/2	2.82	2.17	1.25	0.24	2.50	1.35
B20A2	3.56	2.74	1.58	0.30	3.06	1.70
B20A3	3.32	2.56	1.47	0.28	2.95	1.59
B20A4	4.06	3.12	1.80	0.35	3.60	1.94
B30A1	3.26	2.51	0.64	0.28	1.34	1.56
B30A2	4.57	3.52	0.90	0.39	1.87	2.18
B30A3	3.31	2.55	0.65	0.28	1.36	1.58
B30A4	3.90	3.00	0.77	0.33	1.60	1.86

Limit stresses (kN/cm²)																
Blévot and Frémy [2]		Fusco [15]		Schlaich and Schäfer [14]		ABNT NBR 6118:2014 [2]		EHE-1998 [16]		ACI 318-14 [17]		CEB-*fib* 1990 [18]		CEB-*fib* 2010 [19]		Triple stress state
σ_{zni}	σ_{zns}	σ_{zni}	σ_{zns}	σ_{zni}	σ_{zns}	σ_{zni}	σ_{zns}	σ_{zni}	σ_{zns}	σ_{zni}	σ_{zns}	σ_{zni}	σ_{zns}	σ_{zni}	σ_{zns}	σ_{zns}
2.74	4.80	1.37	0.61	2.19	3.01	1.64	2.33	1.92	8.22	1.64	2.74	1.64	2.33	2.06	2.74	3.83
3.30	5.78	1.65	0.73	2.64	3.63	1.98	2.81	2.31	9.90	1.98	3.30	1.98	2.81	2.48	3.30	4.3
3.55	6.21	1.78	0.79	2.84	3.91	2.13	3.02	2.49	10.65	2.13	3.55	2.13	3.02	2.66	3.55	4.85
3.79	6.63	1.90	0.84	3.03	4.17	2.27	3.22	2.65	11.37	2.27	3.79	2.27	3.22	2.84	3.79	5.14
3.56	6.23	1.78	0.79	2.85	3.92	2.14	3.03	2.49	10.68	2.14	3.56	2.14	3.03	2.67	3.56	4.86
3.10	5.43	1.55	0.69	2.48	3.41	1.86	2.64	2.17	9.30	1.86	3.10	1.86	2.64	2.33	3.10	4.28
4.03	7.05	2.02	0.90	3.22	4.43	2.42	3.43	2.82	12.09	2.42	4.03	2.42	3.43	3.02	4.03	5.44
2.45	4.29	1.23	0.54	1.96	2.70	1.47	2.08	1.72	7.35	1.47	2.45	1.47	2.08	1.84	2.45	3.46
2.46	4.31	1.23	0.55	1.97	2.71	1.48	2.09	1.72	7.38	1.48	2.46	1.48	2.09	1.85	2.46	3.48
Limit stresses average																
3.22	5.64	1.61	0.72	2.58	3.54	1.93	2.74	2.25	9.66	1.93	3.22	1.93	2.74	2.42	3.22	4.43

Table 29
Active stresses × Limits considered for Delalibera and Giongo's [9] tests

Tested model	Active stresses (kN/cm²)					
	Blévot and Frémy [2]		Fusco [15]		Schlaich and Schäfer [14]	
	σ_{zni}	σ_{zns}	σ_{zni}	σ_{zns}	σ_{zni}	σ_{zns}
B35P25E25 and 0	2.91	5.83	1.04	0.65	2.17	2.91
B35P25E25 and 2.5	2.70	5.40	0.96	0.60	2.02	2.70
B35P25E25 and 0A_{swC}	3.01	6.02	1.07	0.67	2.24	3.01
B35P25E25 and 0A_{sw0}	2.25	4.50	0.80	0.50	1.68	2.25
B35P25E25 and 0CG	2.02	4.04	0.72	0.45	1.74	2.02
B45P25E25 and 0	2.75	5.49	1.30	0.61	2.21	3.64
B45P25E25 and 5	2.38	4.76	1.13	0.53	1.92	3.16
B45P25E25 and 0A_{swC}	3.69	7.37	1.75	0.82	2.97	4.89
B45P25E25 and 0A_{sw0}	2.52	5.05	1.19	0.56	2.03	3.34
B45P25E25 and 0CG	2.74	5.48	1.30	0.61	2.46	3.63
B35P50E25 and 0	4.85	9.70	2.22	1.08	3.86	3.10
B35P50E25 and 12.5	4.01	8.01	1.83	0.89	3.19	2.56
B45P50E25 and 0	4.30	8.60	2.39	0.96	3.64	3.34
B45P50E25 and 12.5	3.49	6.98	1.93	0.78	2.95	2.71

Blévot and Frémy [2]		Fusco [15]		Schlaich and Schäfer [14]		ABNT NBR 6118:2014 [2]		EHE-1998 [16]		ACI 318-14 [17]		CEB-*fib* 1990 [18]		CEB-*fib* 2010 [19]		Triple stress state
σ_{zni}	σ_{zns}	σ_{zni}	σ_{zns}	σ_{zni}	σ_{zns}	σ_{zni}	σ_{zns}	σ_{zni}	σ_{zns}	σ_{zni}	σ_{zns}	σ_{zni}	σ_{zns}	σ_{zni}	σ_{zns}	σ_{zns}
4.06	5.68	2.03	0.90	3.25	4.47	2.92	3.45	2.84	12.18	3.25	4.06	2.44	3.45	3.05	4.06	54.8
4.06	5.68	2.03	0.90	3.25	4.47	2.92	3.45	2.84	12.18	3.25	4.06	2.44	3.45	3.05	4.06	5.48
3.28	4.59	1.64	0.73	2.62	3.61	2.36	2.79	2.30	9.84	2.62	3.28	1.97	2.79	2.46	3.28	4.51
3.28	4.59	1.64	0.73	2.62	3.61	2.36	2.79	2.30	9.84	2.62	3.28	1.97	2.79	2.46	3.28	4.51
2.89	4.05	1.45	0.64	2.31	3.18	2.08	2.46	2.02	8.67	2.31	2.89	1.73	2.46	2.17	2.89	4.02
3.10	4.34	1.55	0.69	2.48	3.41	2.23	2.64	2.17	9.30	2.48	3.10	1.86	2.64	2.33	3.10	4.28
3.10	4.34	1.55	0.69	2.48	3.41	2.23	2.64	2.17	9.30	2.48	3.10	1.86	2.64	2.33	3.41	4.28
3.24	4.54	1.62	0.72	2.59	3.56	2.33	2.75	2.27	9.72	2.59	3.24	1.94	2.75	2.43	3.24	4.46
3.24	4.54	1.62	0.72	2.59	3.56	2.33	2.75	2.27	9.72	2.59	3.24	1.94	2.75	2.43	3.24	4.46
2.89	4.05	1.45	0.64	2.31	3.18	2.08	2.46	2.02	8.67	2.31	2.89	1.73	2.46	2.17	2.89	4.02
3.58	5.01	1.79	0.80	2.86	3.94	2.58	3.04	2.51	10.74	2.86	3.58	2.15	3.04	2.69	3.58	4.88
3.51	4.91	1.76	0.78	2.81	3.86	2.53	2.98	2.46	10.53	2.81	3.51	2.11	2.98	2.63	3.51	4.80
3.58	5.01	1.79	0.80	2.86	3.94	2.58	3.04	2.51	10.74	2.86	3.58	2.15	3.04	2.69	3.58	4.88
3.51	4.91	1.76	0.78	2.81	3.96	2.53	2.98	2.46	10.53	2.81	3.51	2.11	2.98	2.63	3.51	4.80
Limit stresses average																
3.38	4.73	1.69	0.75	2.70	3.72	2.43	2.87	2.37	10.14	2.70	3.38	2.03	2.87	2.54	3.38	4.63

Table 30
Active stresses × Limits considered for Barros's [10] tests

Tested model	Active stresses (kN/cm²)					
	Blévot and Frémy [2]		Fusco [15]		Schlaich and Schäfer [14]	
	σ_{zni}	σ_{zns}	σ_{zni}	σ_{zns}	σ_{zni}	σ_{zns}
SR/M1	1.97	3.95	1.20	0.44	1.70	3.36
CR/M8	1.92	3.83	1.15	0.43	1.64	3.22

Blévot and Frémy [2]		Fusco [15]		Schlaich and Schäfer [14]		ABNT NBR 6118:2014 [2]		EHE-1998 [16]		ACI 318-14 [17]		CEB-*fib* 1990 [18]		CEB-*fib* 2010 [19]		Triple stress state
σ_{zni}	σ_{zns}	σ_{zni}	σ_{zns}	σ_{zni}	σ_{zns}	σ_{zni}	σ_{zns}	σ_{zni}	σ_{zns}	σ_{zni}	σ_{zns}	σ_{zni}	σ_{zns}	σ_{zni}	σ_{zns}	σ_{zns}
3.31	4.63	1.66	0.74	2.65	3.64	2.38	2.81	2.32	9.93	2.65	3.31	1.99	2.81	2.48	3.31	4.55
3.31	4.63	1.66	0.74	2.65	3.64	2.38	2.81	2.32	9.93	2.65	3.31	1.99	2.81	2.48	3.31	4.55
Limit stresses average																
3.31	4.63	1.66	0.74	2.65	3.64	2.38	2.81	2.32	9.93	2.65	3.31	1.99	2.81	2.48	3.31	4.55

Table 31
Active stresses × Limits considered for Munhoz's [11] tests

| Tested model | Active stresses (kN/cm²) | | | | | |
| | Blévot and Frémy [2] | | Fusco [15] | | Schlaich and Schäfer [14] | |
	σ_{zni}	σ_{zns}	σ_{zni}	σ_{zns}	σ_{zni}	σ_{zns}
B110P125R1	1.99	3.99	0.99	0.44	1.70	2.76
B110P125R25	2.88	5.76	1.32	0.64	2.41	3.69
B110P125R4	3.93	7.86	1.35	0.87	3.10	3.78
B115P125R1	3.58	7.15	1.63	0.79	2.99	2.28
B115P125R25	4.10	8.20	1.68	0.91	3.35	2.36
B115P125R4	3.44	6.89	1.75	0.77	2.95	2.44
B120P125R1	3.99	7.98	1.94	0.89	3.39	1.81
B120P125R25	4.17	8.34	1.84	0.93	3.46	1.72
B120P125R4	4.39	8.77	2.11	0.97	3.71	1.97
B127P125R1	5.17	10.35	2.35	1.15	4.25	1.65
B127P125R25	5.41	10.81	2.24	1.20	4.34	1.57
B127P125R4	4.79	9.58	2.22	1.06	3.95	1.55

| Limit stresses (kN/cm²) | | | | | | | | | | | | | | | | |
| Blévot and Frémy [2] | | Fusco [15] | | Schlaich and Schäfer [14] | | ABNT NBR 6118:2014 [2] | | EHE-1998 [16] | | ACI 318-14 [17] | | CEB-fib 1990 [18] | | CEB-fib 2010 [19] | | Triple stress state |
σ_{zni}	σ_{zns}	σ_{zni}	σ_{zns}	σ_{zni}	σ_{zns}	σ_{zni}	σ_{zns}	σ_{zni}	σ_{zns}	σ_{zni}	σ_{zns}	σ_{zni}	σ_{zns}	σ_{zni}	σ_{zns}	σ_{zns}
3.05	4.27	1.52	0.68	2.44	3.35	2.19	2.59	2.13	9.14	2.44	3.05	1.83	2.59	2.29	3.05	4.22
3.05	4.27	1.52	0.68	2.44	3.35	2.19	2.59	2.13	9.14	2.44	3.05	1.83	2.59	2.29	3.05	4.22
3.05	4.27	1.52	0.68	2.44	3.35	2.19	2.59	2.13	9.14	2.44	3.05	1.83	2.59	2.29	3.05	4.22
3.05	4.27	1.52	0.68	2.44	3.35	2.19	2.59	2.13	9.14	2.44	3.05	1.83	2.59	2.29	3.05	4.22
3.05	4.27	1.52	0.68	2.44	3.35	2.19	2.59	2.13	9.14	2.44	3.05	1.83	2.59	2.29	3.05	4.22
3.05	4.27	1.52	0.68	2.44	3.35	2.19	2.59	2.13	9.14	2.44	3.05	1.83	2.59	2.29	3.05	4.22
3.05	4.27	1.52	0.68	2.44	3.35	2.19	2.59	2.13	9.14	2.44	3.05	1.83	2.59	2.29	3.05	4.22
3.05	4.27	1.52	0.68	2.44	3.35	2.19	2.59	2.13	9.14	2.44	3.05	1.83	2.59	2.29	3.05	4.22
3.05	4.27	1.52	0.68	2.44	3.35	2.19	2.59	2.13	9.14	2.44	3.05	1.83	2.59	2.29	3.05	4.22
3.05	4.27	1.52	0.68	2.44	3.35	2.19	2.59	2.13	9.14	2.44	3.05	1.83	2.59	2.29	3.05	4.22
3.05	4.27	1.52	0.68	2.44	3.35	2.19	2.59	2.13	9.14	2.44	3.05	1.83	2.59	2.29	3.05	4.22
3.05	4.27	1.52	0.68	2.44	3.35	2.19	2.59	2.13	9.14	2.44	3.05	1.83	2.59	2.29	3.05	4.22
Limit stresses average																
3.05	4.27	1.52	0.68	2.44	3.35	2.19	2.59	2.13	9.14	2.44	3.05	1.83	2.59	2.29	3.05	4.22

Table 32
Active stresses × Limits considered for Mesquita's tests [12]

| Tested model | Active stresses (kN/cm²) | | | | | |
| | Blévot and Frémy [2] | | Fusco [15] | | Schlaich and Schäfer [14] | |
	σ_{zni}	σ_{zns}	σ_{zni}	σ_{zns}	σ_{zni}	σ_{zns}
M	3.88	7.76	1.92	0.86	3.47	5.38

| Limit stresses (kN/cm²) | | | | | | | | | | | | | | | | |
| Blévot and Frémy [2] | | Fusco [15] | | Schlaich and Schäfer [14] | | ABNT NBR 6118:2014 [2] | | EHE-1998 [16] | | ACI 318-14 [17] | | CEB-fib 1990 [18] | | CEB-fib 2010 [19] | | Triple stress state |
σ_{zni}	σ_{zns}	σ_{zni}	σ_{zns}	σ_{zni}	σ_{zns}	σ_{zni}	σ_{zns}	σ_{zni}	σ_{zns}	σ_{zni}	σ_{zns}	σ_{zni}	σ_{zns}	σ_{zni}	σ_{zns}	σ_{zns}
4.22	5.91	2.11	0.94	3.38	4.64	3.04	3.59	2.95	12.66	3.38	4.22	2.53	3.59	3.17	4.22	5.68

Table 33
Active stresses × Limits considered for Cao and Bloodworth's [13] tests

Tested model	Active stresses (kN/cm²)					
	Blévot and Frémy [2]		Fusco [15]		Schlaich and Schäfer [14]	
	σ_{zni}	σ_{zns}	σ_{zni}	σ_{zns}	σ_{zni}	σ_{zns}
B4A1	6.25	6.64	0.80	3.69	4.09	1.18
B4A2	4.37	4.64	0.74	2.58	3.03	1.10
B4A3	6.02	6.39	1.24	3.55	4.34	1.84
B4A4	6.23	6.62	1.42	3.68	4.58	2.10
B4A5	6.04	6.41	1.67	3.56	4.61	2.49
B4B2	6.59	5.38	0.96	3.89	4.52	1.10
B4B3	8.01	5.67	1.03	4.73	5.37	1.03

Limit stresses (kN/cm²)																	
Blévot and Frémy [2]		Fusco [15]		Schlaich and Schäfer [14]		ABNT NBR 6118:2014 [2]		EHE-1998 [16]		ACI 318-14 [17]		CEB-*fib* 1990 [18]		CEB-*fib* 2010 [19]		Triple stress state
σ_{zni}	σ_{zns}	σ_{zni}	σ_{zns}	σ_{zni}	σ_{zns}	σ_{zni}	σ_{zns}	σ_{zni}	σ_{zns}	σ_{zni}	σ_{zns}	σ_{zni}	σ_{zns}	σ_{zni}	σ_{zns}	σ_{zns}
2.03	4.26	1.02	0.45	1.62	2.23	1.22	1.73	1.42	6.09	1.22	2.03	1.22	1.73	1.52	2.03	2.92
2.18	4.58	1.09	0.48	1.74	2.40	1.3	1.85	1.53	6.54	1.31	2.18	1.31	1.85	1.64	2.18	3.12
2.43	5.10	1.22	0.54	1.94	2.67	1.46	2.07	1.70	7.29	1.46	2.43	1.46	2.07	1.82	2.43	3.44
2.44	5.12	1.22	0.54	1.95	2.68	1.46	2.07	1.71	7.32	1.46	2.44	1.46	2.07	1.83	2.44	3.45
2.30	4.83	1.15	0.51	1.84	2.53	1.38	1.96	1.61	6.90	1.38	2.30	1.38	1.96	1.73	2.30	3.27
2.56	5.38	1.28	0.57	2.05	2.82	1.54	2.18	1.79	7.68	1.54	2.56	1.54	2.18	1.92	2.56	3.60
2.47	5.19	1.24	0.55	1.98	2.72	1.48	2.10	1.73	7.41	1.48	2.47	1.48	2.10	1.85	2.47	3.49
Limit stresses average																
2.34	4.92	1.17	0.52	1.88	2.58	1.41	1.99	1.64	7.03	1.41	2.34	1.41	1.99	1.76	2.34	3.33
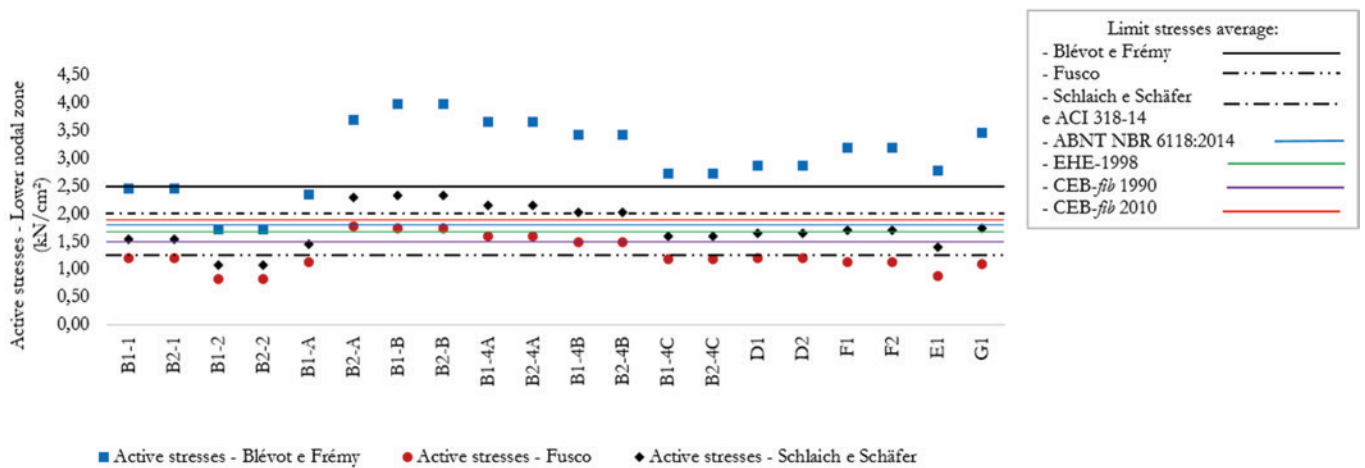
Figure 7
Models tested by Mautoni [5] × σ_{zni}
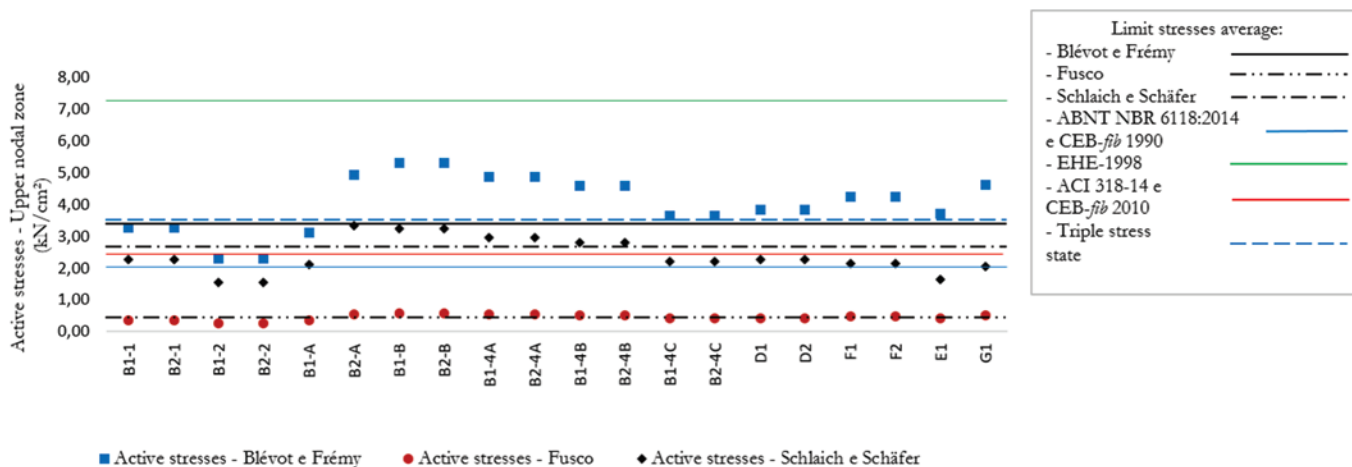
Figure 8
Models tested by Mautoni [5] × σ_{zns}
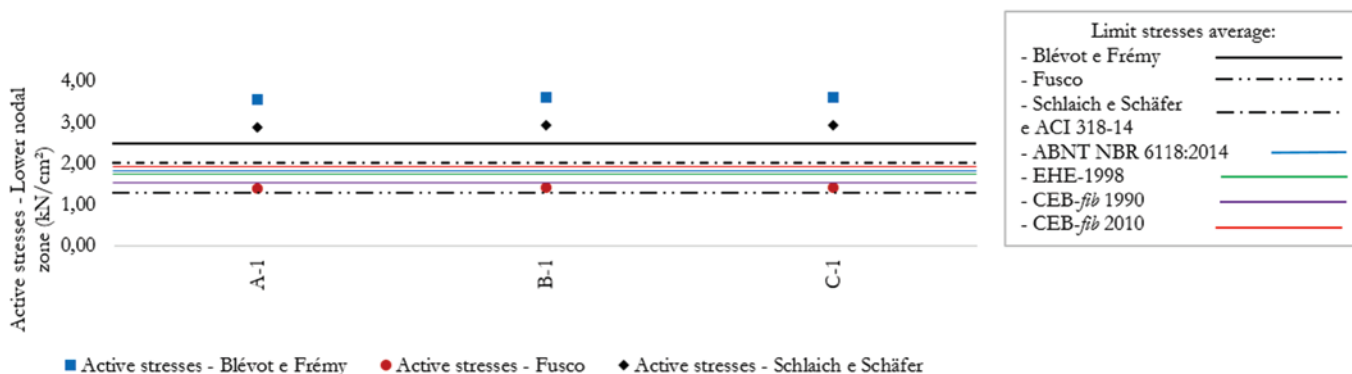
Figure 9
Models tested by Fusco [6] × σ_{zni}
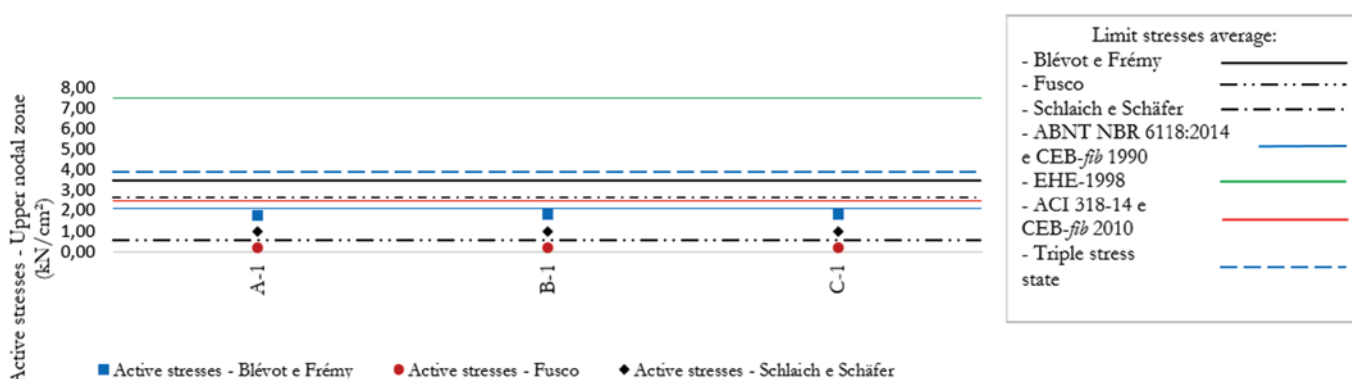
Figure 10
Models tested by Fusco [6] × σ_{zns}
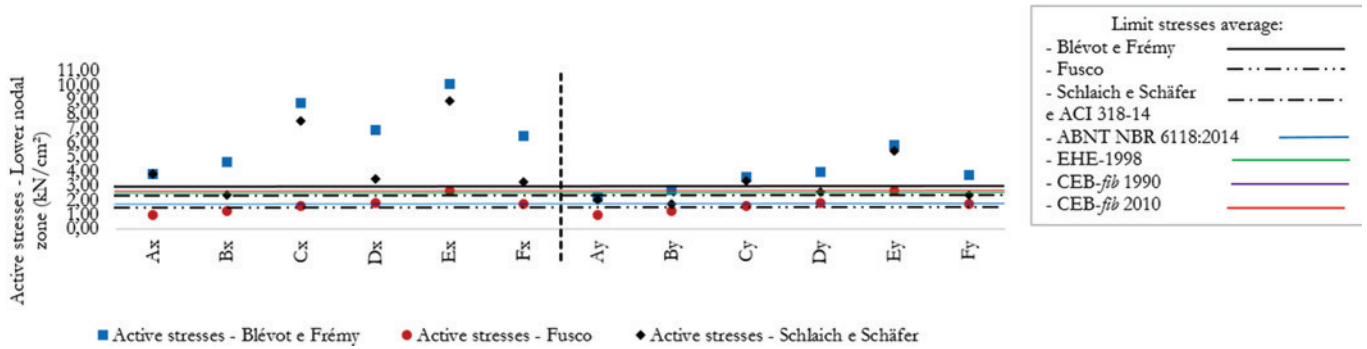
Figure 11
Models tested by Adebar et al. [4] × σ_{zni}
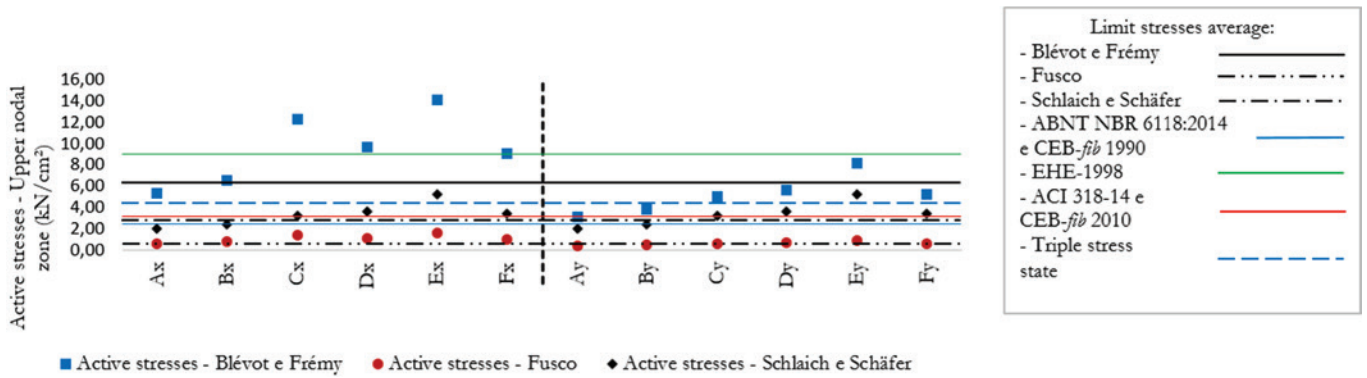
Figure 12
Models tested by Adebar et al. [4] × σ_{zns}
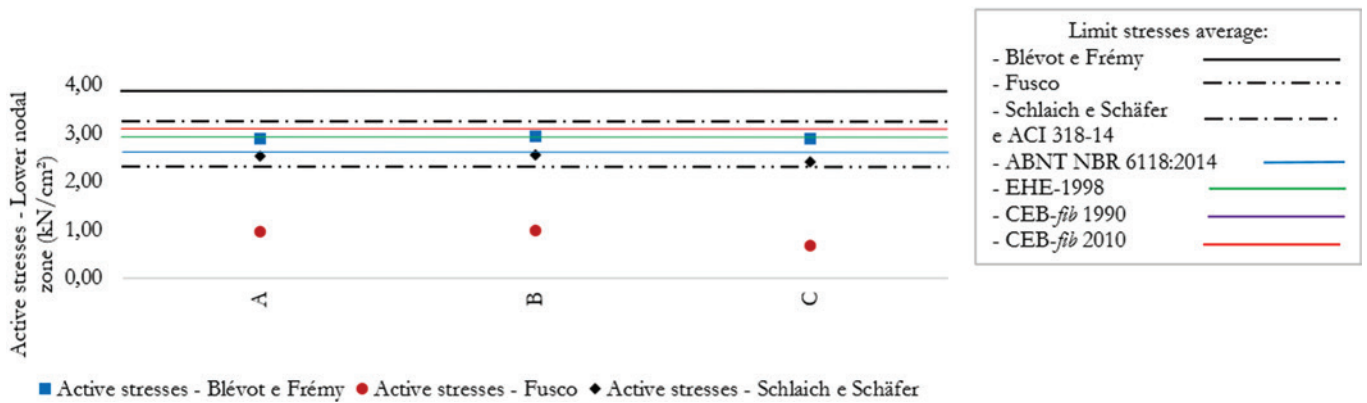
Figure 13
Models tested by Chan and Poh [7] × σ_{zni}
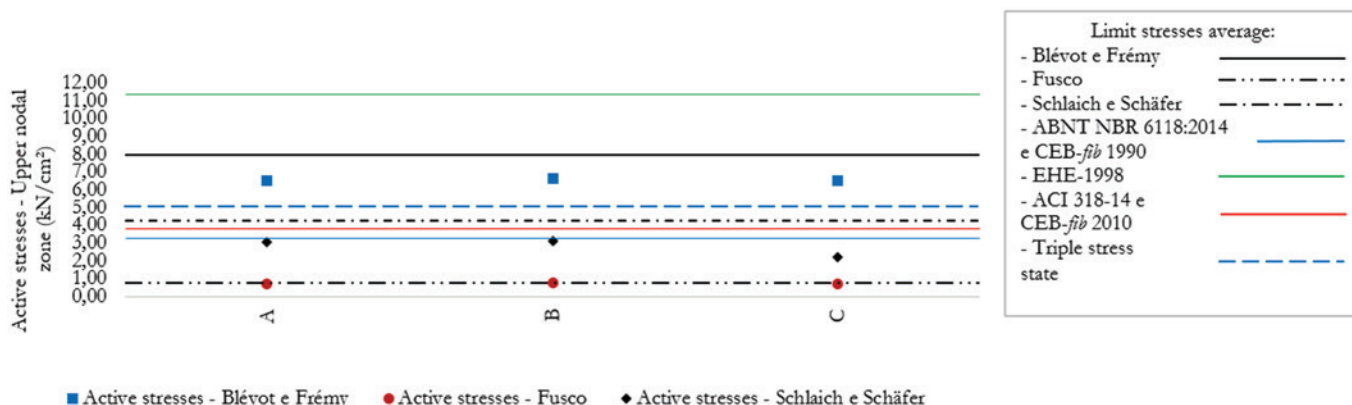
Figure 14
Models tested by Chan and Poh [7] × σ_{zns}
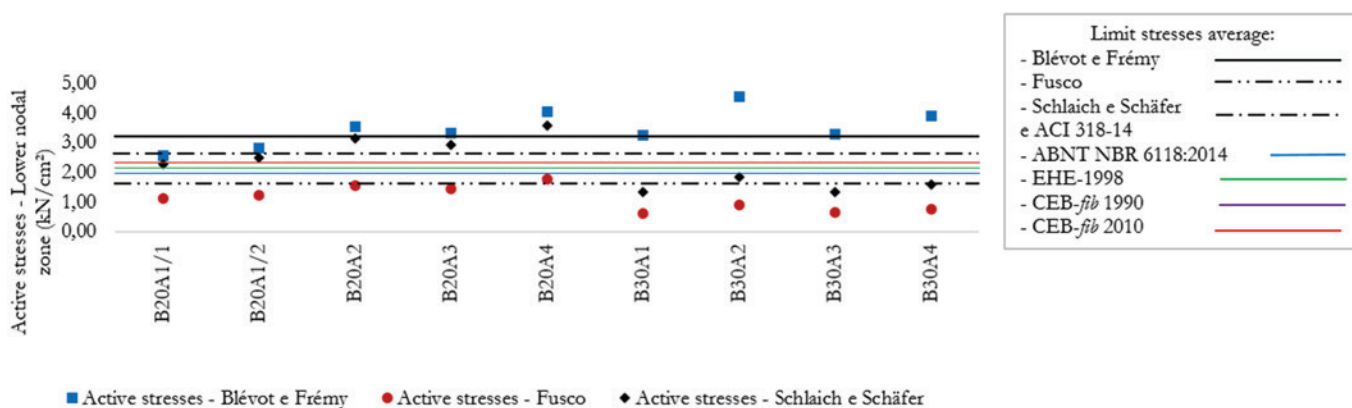
Figure 15
Moldels tested by Miguel [8] × σ_{zni}
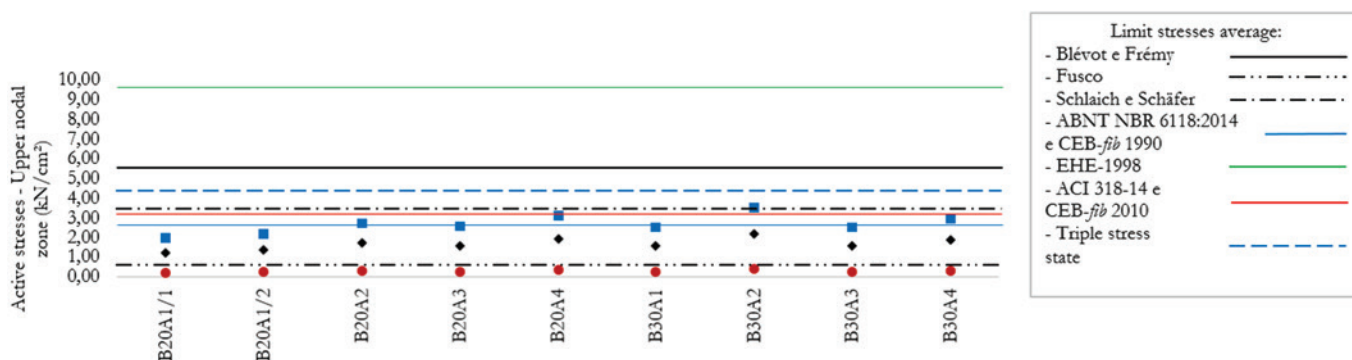
Figure 16
Models tested by Miguel [8] × σ_{zns}
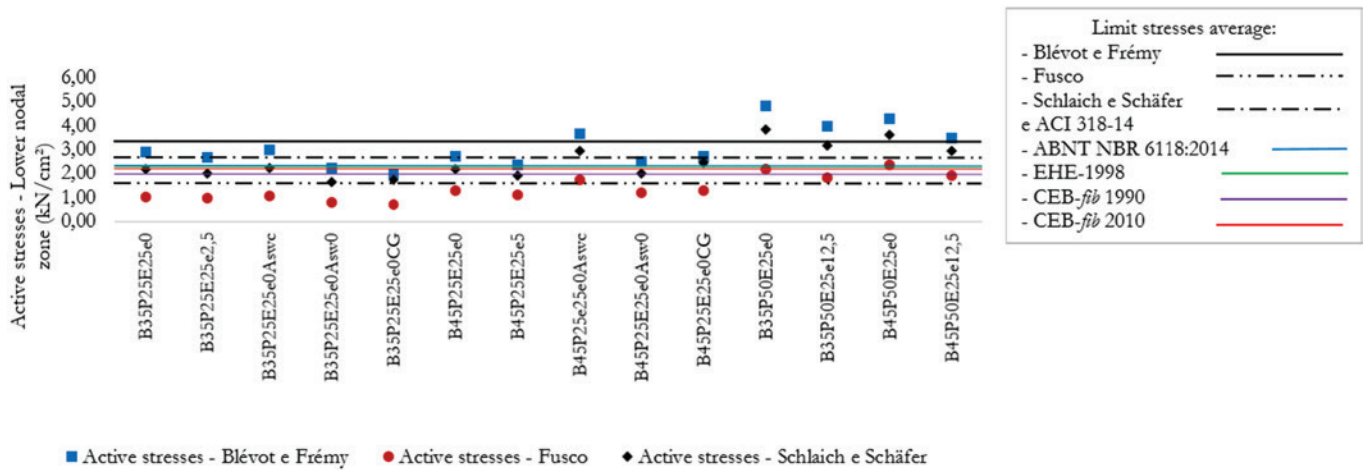
Figure 17
Models tested by Delalibera and Giongo [9] × σ_{zni}
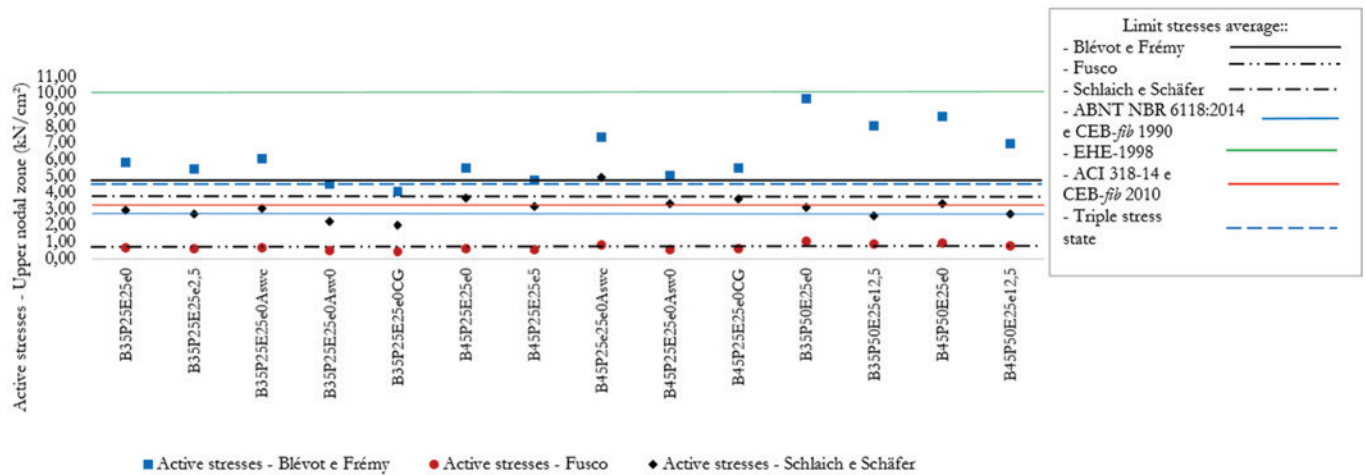
Figure 18
Models tested by Delalibera and Giongo [9] × σ_{zns}
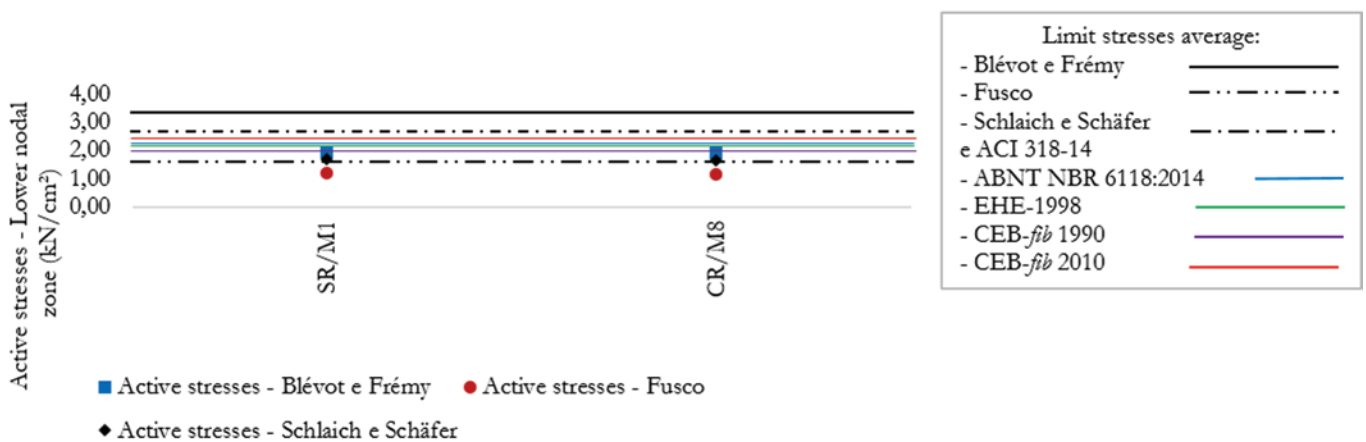
Figure 19
Models tested by Barros [10] × σ_{zni}
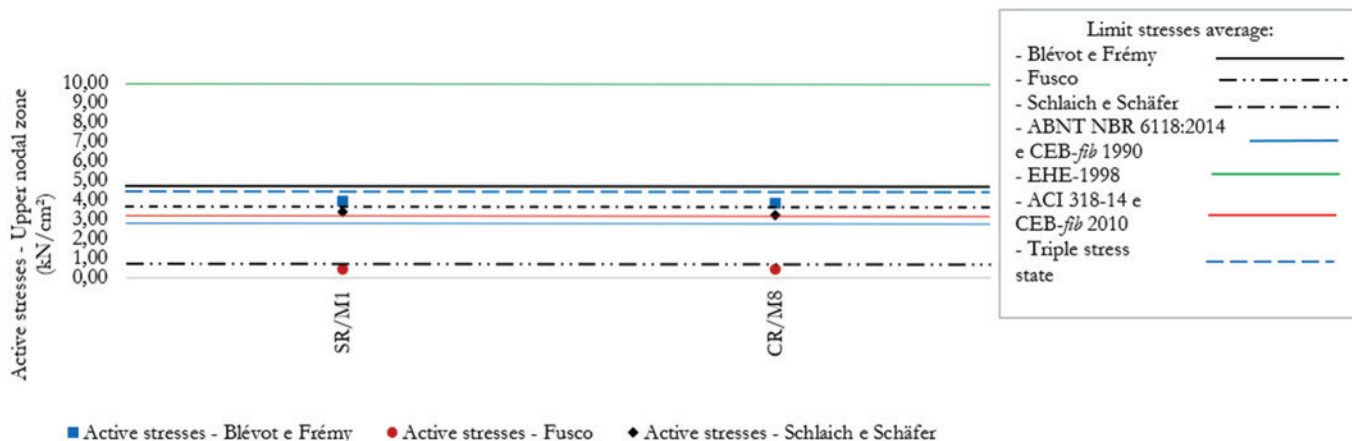
Figure 20
Models tested by Barros [10] × σ_{zns}
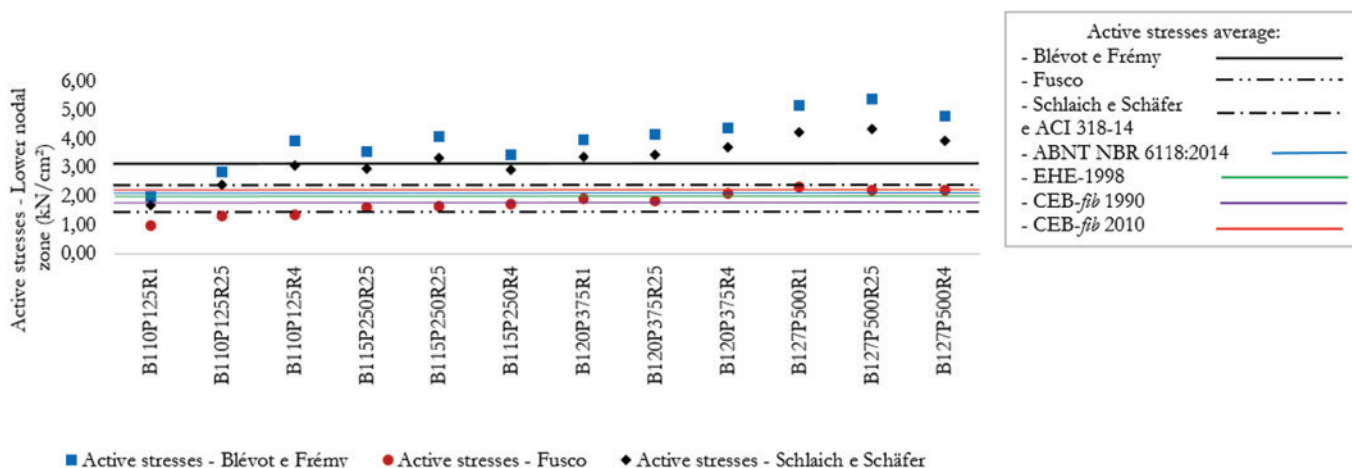
Figure 21
Models tested by Munhoz [11] × σ_{zni}
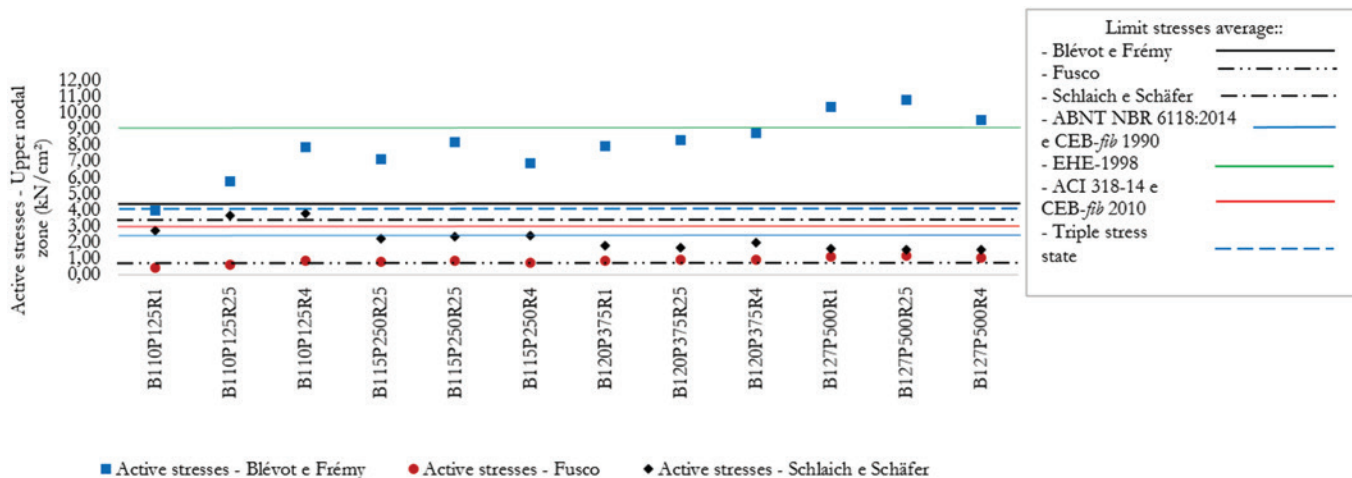
Figure 22
Models tested by Munhoz [11] × σ_{zns}
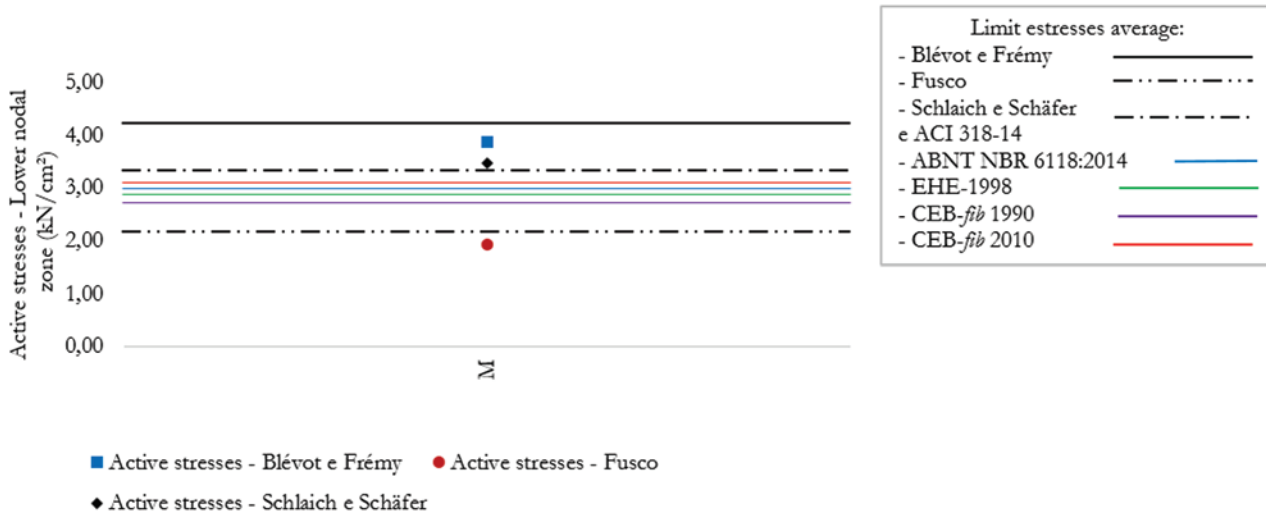
Figure 23
Models tested by Mesquita [12] × σ_{zni}
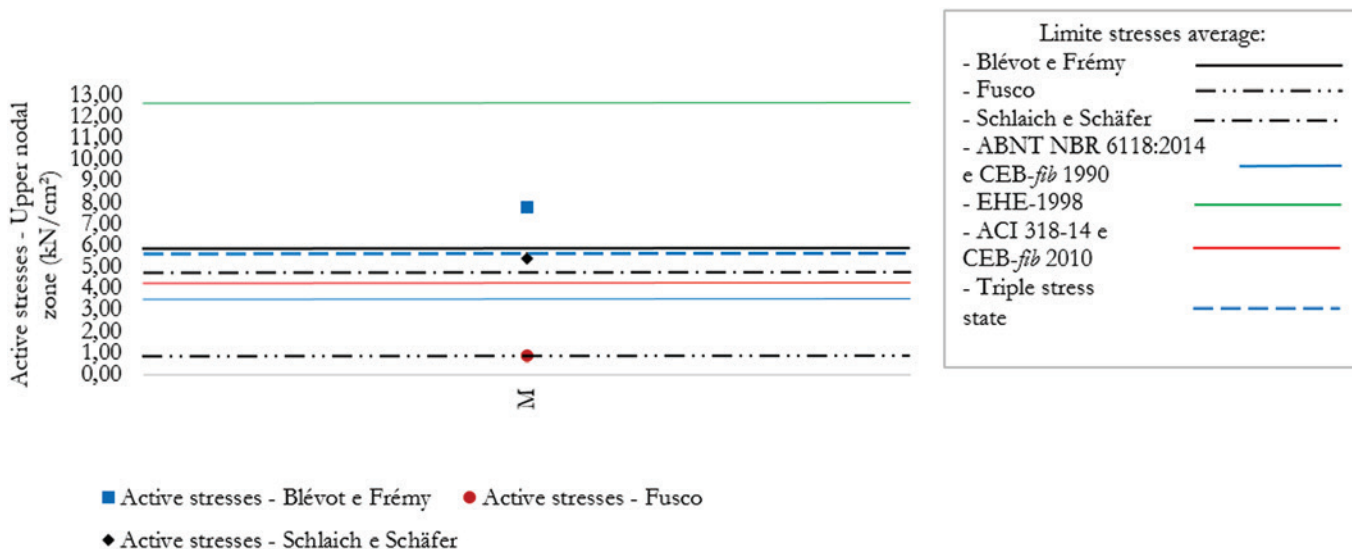
Figure 24
Models tested by Mesquita [12] × σ_{zns}
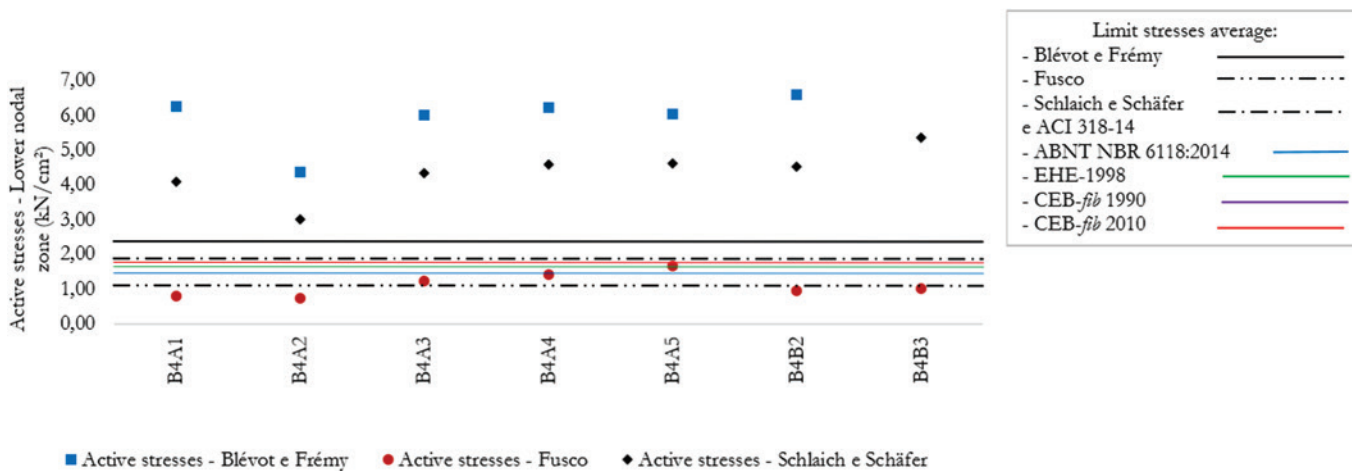
Figure 25
Models tested by Cao and Bloodworth [13] × σ_{zni}
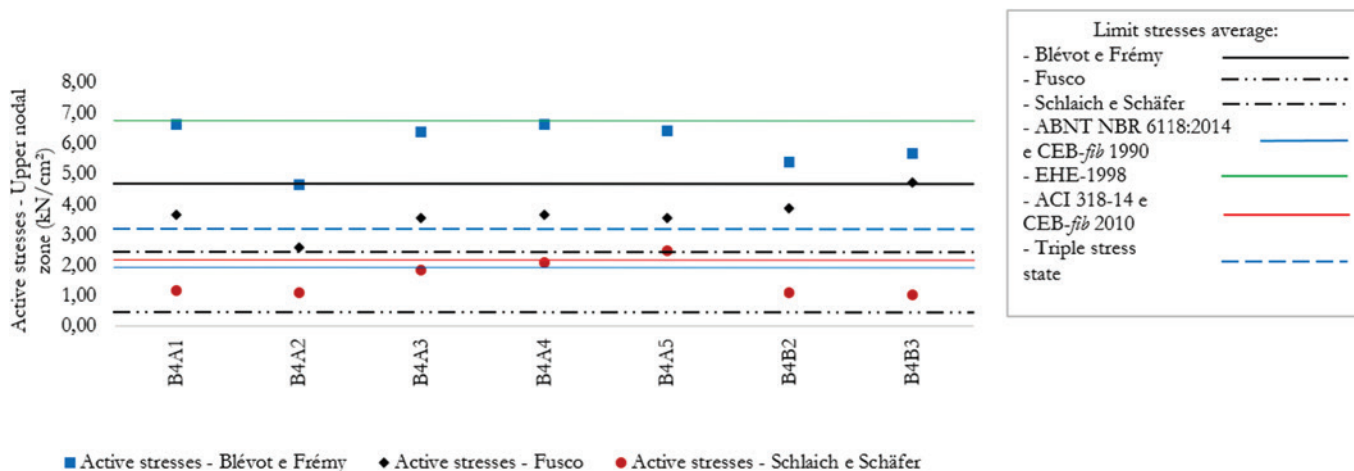
Figure 26
Models tested by Cao and Bloodworth [13] × σ$_{zns}$
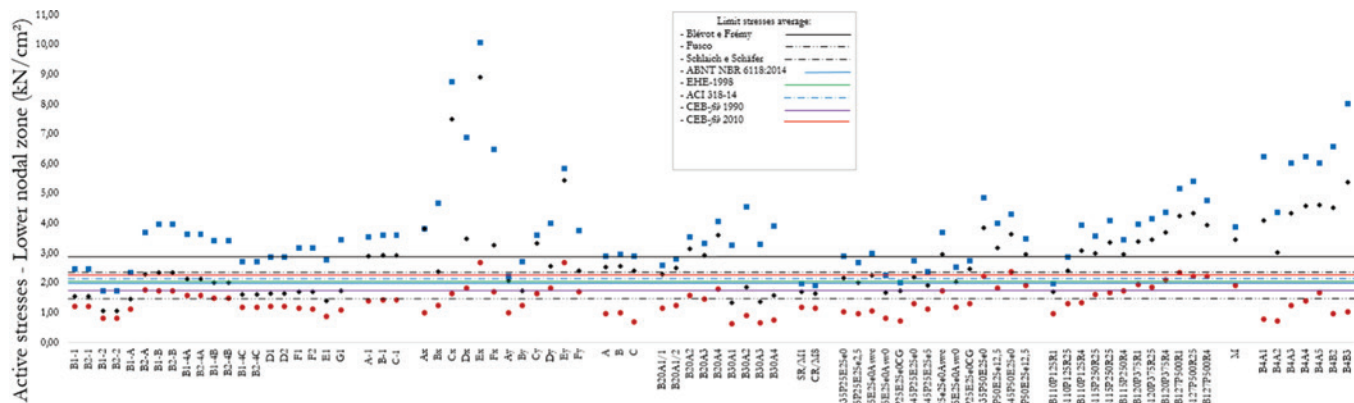
Figure 27
Models tested × σ$_{zni}$
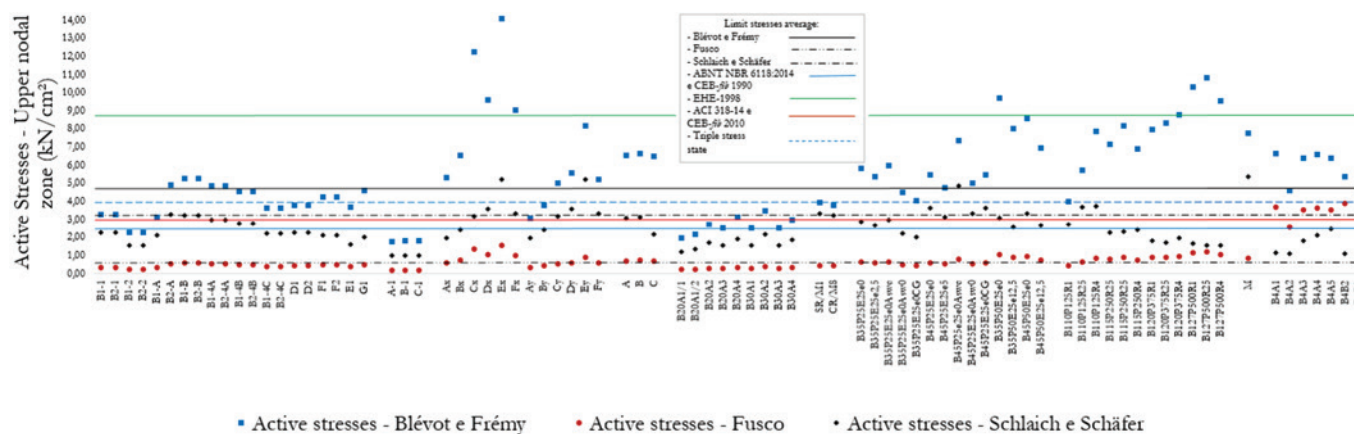
Figure 28
Models tested × σ$_{zns}$

that were much smaller than the limit value presented by the Spanish standard.

By evaluating the graphs of stresses (excluding the values obtained by using the model proposed by Fusco [15]) it is shown that, for the lower nodal area, the results fit better with the limits suggested by the CEB-*fib* [18], while for the upper nodal zone, the results fit better with the limits indicated by Schlaich and Schäfer [14] and by the triple stress state proposed by the authors of this work. This confirms that, in addition with the analysis of Figure [4], the node representation for the upper nodal zone suggested by Schlaich and Schäfer [14] is best characterized by the triple stress state. Thus, it is suggested that for the upper nodal zone the effect of the multiaxial stress state should be considered.

Different areas of cross sections of columns, existence of reinforcement to absorb tensile stresses on the struts, cross section of the pile and column reinforcement ratio, affect the values of the operating stresses and are not contemplated by any calculation model presented so far, being possible source for future research.

5. Acknowledgments

6. References

[1] BLÉVOT, J. Semelles en béton armé sur pieux. Institut de Recherches Appliquées du Béton Armé. Paris, m. 111-112, 1957.

[2] BLÉVOT, J.; FRÉMY, R. Semelles sur pieux. Analles d'Institut Techique du Bâtiment et des Travaux Publics. Paris, v.20, n. 230, 1967, p. 223-295.

[3] ASSOCIAÇÃO BRASILEIRA DE NORMAS TÉCNICAS (2014). ABNT NBR 6118:2014 – Projeto de estruturas de concreto. Rio de Janeiro: ABNT 2014.

[4] ADEBAR, P.; KUCHMA, D. COLLINS, M. P. Strut-and-tie models for design of pile caps: an experimental study. ACI Journal, v.87, 1990; p.81-91.

[5] MAUTONI, M. Blocos sobre dois apoios, São Paulo, Grêmio Politécnico, 1972, 89 p.

[6] FUSCO, P. B. Investigação experimental sobre o valor limite T_{wu} das tensões de cisalhamento no concreto estrutural, São Paulo, 1985.

[7] CHAN, T. K. POH, C. K. Behavior of precast reinforced concrete pile caps. Construction and building materials, v.14, n.2, 2000; p.73-78.

[8] MIGUEL, M. G. Análise numérica e experimental de blocos sobre três estacas, São Carlos, 2000, Tese (doutorado) – Escola de Engenharia de São Carlos, Universidade de São Paulo, 242 p.

[9] DELALIBERA, R. G.; GIONGO, J. S. Deformação nas diagonais comprimidas em blocos sobre duas estacas. Revista IBRACON de estruturas e materiais. V1, n.2 (junho 2008), p. 121-157.

[10] BARROS, R. Análise numérica e experimental de blocos de concreto armado sobre duas estacas com cálice externo, par-

cialmente embutido e embutido utilizado na ligação pilar-fundação, São Carlos, 2013, Tese (doutorado) – Escola de Engenharia de São Carlos, Universidade de São Paulo, 355 p.

[11] MUNHOZ, F. S. Análise experimental e numérica de blocos rígidos sobre duas estacas com pilares de seções quadradas e retangulares e diferentes taxas de armadura, São Carlos, 2014, Tese (doutorado) – Escola de Engenharia de São Carlos, Universiadade de São Paulo, 358 p.

[12] MESQUITA, A. C. A influência da ligação pilar-bloco nos mecanismos de rupture de blocos de fundação sobre duas estacas, Goiânia, 2015, Dissertação (mestrado) – Universidade Federal de Goiás, 165 p.

[13] CAO, J.; BLOODWORTH, A. G. Shear capacity of reinforced concrete pile caps. At IABSE (International Associatoin for bridge and structural engineering). Germany, 2007.

[14] SCHLAICH, J.; SCHÄFER, K. Design and detailing of structural concrete using strut-and-tie models, The Structural Engineer, v.69, n.6, 1991, p. 113-125.

[15] FUSCO, P. B. Técnicas de armar estruturas de concreto, 2 ed, São Paulo-SP, Editora Pini LTDA, 2013, 395 p.

[16] COMISÍON PERMANETE DEL HERMIGÓN (1998). Ministério de Fomento. Centro de Publicaciones. Instricción de Hormigón Estructural (EHE), Madrid, 1998.

[17] AMERICAN CONCRETE INSTITUTE 920140. Building code requirements for structural concrete (ACI 318-14). Detroit, USA.

[18] COMITE EURO-INTERNACIONAL DU BÉTON (1990). CEB-FIB Model Code. Paris, 1990.

[19] COMITE EURO-INTERNACIONAL DU BÉTON (2010). CEB-FIB Model code prepared by special activity group 5. Paris, 2010.

[20] INSTITUTO BRASILEIRO DO CONCRETO. ABNT NBR 6118:2014 Comentários e Exemplos de Aplicação. 1 ed, São Paulo-SP, 2015, 480 p.